AFCRL-68-0083

MULTIPACTOR DISCHARGE EXPERIMENTS

By

EDWARD F. VANCE JOSEPH E. NANEVICZ

CONTRACT AF 19(628)-4800
PROJECT NO. 4600
TASK NO. 460010
WORK UNIT NO. 46001001

Scientific Report 5

December 1967

Contract Monitor: CHARLES E. ELLIS
MICROWAVE PHYSICS LABORATORY

Prepared for

AIR FORCE CAMBRIDGE RESEARCH LABORATORIES
OFFICE OF AEROSPACE RESEARCH
UNITED STATES AIR FORCE
BEDFORD, MASSACHUSETTS 01730

STANFORD RESEARCH INSTITUTE

MENLO PARK, CALIFORNIA

61

UNCLASSIFIED

Security Classification

DOCUMENT CONTROL DATA - R & D

(Security classification of title, body of abstract and indexing annotation must be entered when the overall report is classified)

1 ORIGINATING ACTIVITY (Corporate author) Stanford Research Institute 333 Ravenswood Avenue Menlo Park, California 94025	2a. REPORT SECURITY CLASSIFICATION UNCLASSIFIED 2b. GROUP n/a

3 REPORT TITLE

MULTIPACTOR DISCHARGE EXPERIMENTS

4 DESCRIPTIVE NOTES (Type of report and inclusive dates)

Scientific. Interim.

5 AUTHOR(S) (First name, middle initial, last name)

Edward F. Vance
Joseph E. Nanevicz

6 REPORT DATE	7a. TOTAL NO OF PAGES	7b. NO OF REFS
December 1967	69	34

8a CONTRACT OR GRANT NO	9a. ORIGINATOR'S REPORT NUMBER(S)
AF 19(628)-4800 b PROJECT NO Task, Work Unit Nos. 4600-10-01 c DoD Element 62405304 d DoD Subelement 674600	Scientific Report 5, SRI Project 5359 9b. OTHER REPORT NO(S) (Any other numbers that may be assigned this report) AFCRL-68-0083

10 DISTRIBUTION STATEMENT

This document is subject to special export controls and each transmittal to foreign governments or foreign nationals may be made only with prior approval of AFCRL (CRDM), L.G. Hanscom Field, Bedford, Massachusetts 01730

11 SUPPLEMENTARY NOTES	12 SPONSORING MILITARY ACTIVITY
TECH, OTHER	Air Force Cambridge Research Laboratories (CRD) L. G. Hanscom Field Bedford, Massachusetts 01730

13 ABSTRACT

An experimental investigation of the multipactor discharge mechanism was conducted to determine the effect of dc bias, electrode materials, and electrode geometry on the RF voltage required for initiation of the discharge. The experiments showed that most of the commonly used aerospace materials support multipactor discharges, and that the discharge can occur over a wide range of bias voltages. The experiments were conducted with a parallel-plate geometry, a coaxial geometry and with the cone-plane configuration of a discone antenna. All of the coaxial electrode geometries supported multipactor discharges, and the discone configurations with cone half-angles greater than 60 degrees supported the discharges. Attempts to measure the RF power dissipated by the discharge indicated that this power was relatively small, so the main detrimental effect of the multipactor discharge on RF systems in space will be in detuning high-Q circuits and in the possibility of more serious failure mechanisms being induced by the multipactor discharge.

DD FORM 1 NOV 65 1473 (PAGE 1)

S/N 0101-807-6801

UNCLASSIFIED

Security Classification

14 KEY WORDS	LINK A		LINK B		LINK C	
	ROLE	WT	ROLE	WT	ROLE	WT
Multipactor discharge RF breakdown Spacecraft antennas Vacuum breakdown						

STANFORD RESEARCH INSTITUTE
MENLO PARK, CALIFORNIA

AFCRL-68-0083

MULTIPACTOR DISCHARGE EXPERIMENTS

By

EDWARD F. VANCE JOSEPH E. NANEVICZ

SRI Project 5359

CONTRACT AF 19(628)-4800
PROJECT NO. 4600
TASK NO. 460010
WORK UNIT NO. 46001001

Scientific Report 5

December 1967

Contract Monitor: CHARLES E. ELLIS
MICROWAVE PHYSICS LABORATORY

Approved: TETSU MORITA, MANAGER
ELECTROMAGNETIC SCIENCES LABORATORY

D. R. SCHEUCH, EXECUTIVE DIRECTOR
ELECTRONICS AND RADIO SCIENCES

Prepared for

AIR FORCE CAMBRIDGE RESEARCH LABORATORIES
OFFICE OF AEROSPACE RESEARCH
UNITED STATES AIR FORCE
BEDFORD, MASSACHUSETTS 01730

Copy No. 20

ABSTRACT

An experimental investigation of the multipactor discharge mechanism was conducted to determine the effect of dc bias, electrode materials, and electrode geometry on the RF voltage required for initiation of the discharge in components of RF systems used in space. The experiments showed that most of the commonly used aerospace materials support multipactor discharges, and that the discharge can occur over a wide range of bias voltages. The experiments were conducted with a parallel-plate geometry, a coaxial geometry, and the cone-plane configuration of a discone antenna. All of the coaxial electrode geometries supported multipactor discharges, and the discone configurations with cone half-angles greater than 60 degrees supported the discharges. Attempts to measure the RF power dissipated by the discharge indicated that this power was relatively small, so the main detrimental effect of the multipactor discharge on RF systems in space will be in detuning high-Q circuits and in the possibility of more serious failure mechanisms being induced by the multipactor discharge.

CONTENTS

FOREWORD

This report was prepared by Stanford Research Institute (SRI), Menlo Park, California, and is the fifth in a series of Scientific Reports issued under Air Force Contract AF 19(628)-4800, Project No. 4600, Task No. 460010. The work was administered under the Office of Aerospace Research of the Air Force Cambridge Research Laboratories. Mr. Charles Ellis was the Air Force task engineer.

The report presents the results of a study of a particular topic in the general area of problems associated with the radiation and reception of electromagnetic energy from aircraft and guided missiles. The principal investigator, Dr. J. E. Nanevicz, was responsible for research activity under Stanford Research Institute Project 5359.

With the publication of this report, the Scientific Reports issued in this series to date are as follows:

Scientific Report 1

"An Experimental Study of Non-Linear Plasma-Wave Interaction," by W. C. Taylor, AFCRL-65-654 (August 1965).

Scientific Report 2

"Rocket Motor Charging Experiments," by E. F. Vance and J. E. Nanevicz, AFCRL-66-497 (June 1966).

Scientific Report 3

"SRI Participation in Voltage Breakdown and Rocket Charging Experiments on AFCRL Nike-Cajun Rocket AD 6.841," by J. E. Nanevicz, J. B. Chown, E. F. Vance, and J. A. Martin. AFCRL-66-588 (August 1966).

Scientific Report 4

"Measurement of RF Ionization Rates in High-Temperature Air," by W. C. Taylor, J. B. Chown, and T. Morita AFCRL-67-028 (March 1967).

Scientific Report 5

"Multipactor Discharge Experiments," by E. F. Vance and J. E. Nanevicz (December 1967).

ILLUSTRATIONS

TABLES

BLANK PAGE

I INTRODUCTION

A. Background

At air pressures encountered in the lower atmosphere, electrical breakdown is dependent on gas processes to produce some or all of the free charge involved in the discharge. The maximum power that can be handled before breakdown occurs is thus a function of pressure. According to classical theory of gaseous discharge, breakdown voltage decreases with decreasing pressure until a minimum breakdown voltage is obtained. Further decreases in pressure then cause the breakdown voltage to increase because the reduced collision frequency must be compensated for by a higher probability that a collision will be an ionizing one, implying a higher electron energy or a larger accelerating field.[1]* As the pressure is reduced below the value associated with minimum breakdown voltage, therefore, the breakdown voltage may increase rapidly, as suggested by the dashed curve of Fig. 1.

For RF voltages, however, the multipactor breakdown mechanism may become effective when the mean-free-path is of the order of the electrode spacing or greater. This breakdown mechanism occurs when electrons are accelerated across a gap during one half-cycle and strike the electrode with sufficient energy to produce secondary emission. Each of these secondary electrons is then accelerated back across the gap during the succeeding half-cycle, producing more secondary electrons when they strike. The number of electrons participating in the discharge thus increases until the electrons are lost by diffusion or phase dispersion as fast as they are produced by secondary emission at the electrodes. For the multipactor mechanism to operate, the coefficient of secondary emission must be greater than 1.0, and the frequency, voltage, and path length must be such that the electron transit time is approximately half the RF period, or some odd multiple of a half period. Because the participating free charge is supplied by the electrodes, multipactor dis-

*References are listed at the end of the text.

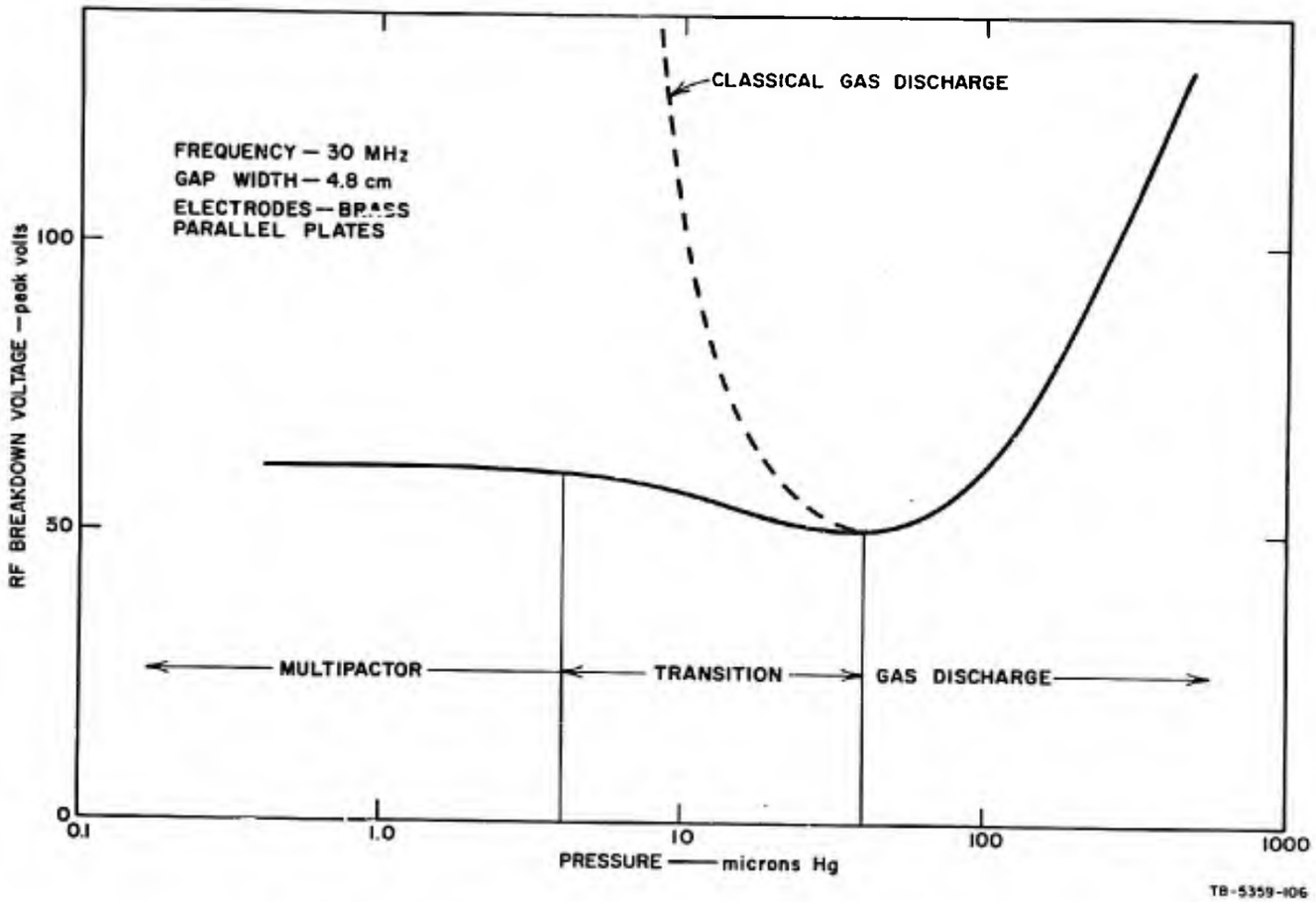

FIG. 1 VARIATION OF RF BREAKDOWN VOLTAGE WITH PRESSURE

charge is independent of the type of gas or the pressure, so long as the pressure is low enough that the probability of an electron colliding with a gas molecule during one transit is low.

The solid curve of Fig. 1 shows the measured breakdown voltage for a parallel-plate-gap as pressure was reduced. At pressures above 60 microns Hg the breakdown curve is the classical gas discharge Paschen curve. Because of the gap width and frequency used in this experiment, the breakdown voltage did not follow the dashed curve on the low-pressure side of the minimum, but, instead, increased slowly to a plateau defined by the multipactor breakdown voltage for this gap width and frequency. Had the gap width or frequency been larger, the breakdown voltage along the plateau would have been higher. Krebs has demonstrated this variation of plateau height with gap-width at microwave frequencies.[2] The variation of multipactor breakdown voltage in a parallel-plate gap with frequency and gap-width has also been described by Hatch and Williams.[3,4]

Since the multipactor discharge depends on secondary emission at the electrodes, the discharge can occur from insulating surfaces as well as from conductors. Indeed, since many insulators have higher secondary-emission coefficients than conductors, multipacting may occur more readily from the insulators. The multipactor discharge is also unique in that there is a lower threshold voltage below which the discharge cannot occur, and an upper threshold voltage above which the discharge does not occur. In addition, for a given path length, there exists a cutoff frequency below which the discharge does not occur. The discharge is thus frequency- and voltage-selective; however, multipactor discharges can occur over a wide range of frequencies and voltages above the cutoff frequency. Furthermore, in a configuration where more than one path length is available, less frequency selectivity would be expected.

B. Objective of This Study

Although considerable research has been conducted on multipactor discharges, the effort prior to the 1960's has been directed primarily toward (1) understanding the physics of the discharge and (2) preventing the deleterious effects of the discharge in microwave tubes, cavities, etc.

In the first category, experiments were conducted in parallel-plate geometries because these are easy to analyze and understand, while in the latter category, the primary effort was devoted to recognizing the conditions under which the discharge occurs and eliminating these conditions.

With the advent of satellities and spacecraft, however, broader interest in the multipactor discharge mechanism has developed since, in the space environment, multipactor discharges can occur at any frequency if the proper geometry is provided. Thus multipactor discharges at the lower VHF and HF frequencies, which do not normally occur in microwave tubes because of the small size of the electrodes, could pose a problem on spacecraft where connectors, cavities, and antennas are all exposed to the high-vacuum environment.

The purpose of the work described here was, therefore, to investigate the ramifications of the multipactor discharge as a voltage-breakdown mechanism that might occur in spacecraft RF systems such as coaxial conductors and antennas.

C. Nature of Experiments

To investigate these ramifications of the multipactor discharge mechanism, experiments were conducted at the VHF and HF frequencies with electrode geometries representative of those found in typical RF components. The principal geometries studied were parallel plates, coaxial cylinders, and cone-plane electrode configurations. Experiments were conducted primarily to measure upper and lower breakdown threshold potentials and the limitations imposed by electrode geometry, but, in selected experiments, attempts were also made to measure the power dissipated in the discharge.

The experiments in the uniform field were conducted to explore the region over which multipactor discharges would occur in the presence of dc bias, and to examine the effect of electrode materials on the discharge. The results of these experiments indicate that the discharge occurs over a considerable range of bias voltages, and that for moderate

bias voltages, the threshold voltage for multipactor discharges is reduced, rather than increased. The discharge was found to occur with practically all common metal electrode materials except pure titanium (but titanium alloy has been found by others to support multipactor discharges).

In the coaxial geometry, multipactor discharges will occur for electrode diameter ratios from 1 (parallel plane) to as large as 97. The discharge in a coaxial geometry is also supported in the presence of a large range of dc bias values, and a large region of one-sided multipactor discharge is apparent when bias is applied.

The experiments with discone antenna configurations indicated that multipactor discharges occur in the configurations with large cone angles, but in practical discone antenna sizes the discharge is confined to a small region about the feed point where the electron path length is suitable for multipacting. The power absorbed by the discharge appears to be small compared to the radiated power. Measurements of power dissipated in the coaxial discharge were also attempted, but these measurements were difficult because the power dissipated in the discharge was so small that it was masked by circuit power losses and instrumentation accuracy. These experiments indicate that the power lost in the multipactor discharge is a problem mainly when the discharge occurs in a high-Q tuned circuit, when it causes electrode heating, or when it induces a more drastic failure mechanism such as a gas discharge or an arc.

BLANK PAGE

II MULTIPACTOR DISCHARGE IN A UNIFORM FIELD

A. General

The physics of the multipactor discharge in the uniform field between parallel plates has been investigated extensively by others.[2-16] There appears to be general agreement on the basic concept of the discharge mechanism and on the trends of the variation of threshold voltages with frequency and gap width. There has been some controversy between the followers of Hatch and Williams and the followers of Krebs over the proper assumptions regarding the relation of the impact velocity to the velocity of emission for the electrons. Hatch and Williams assumed the ratio k of these velocities to be constant, and have developed considerable evidence supporting this assumption. Krebs on the other hand has performed an extensive and rigorous analysis of the ballistics of electrons in the discharge and concludes that k cannot be constant. Krebs' analysis appears to be more thorough and complete, but is also more cumbersome to use. For those whose interest is primarily in the effects of the discharge, rather than in precise analysis of the physics of the discharge, therefore, the simpler Hatch and Williams theory appears to be satisfactory.

Contours from Hatch and Williams[4] of theoretical breakdown voltage as a function of the frequency-gap-width product fd are illustrated by the solid curves of Fig. 2 for the first three modes of multipactor discharge. These curves are based on the assumption that $k = 3$, the lower breakdown emission phase Φ_ℓ is 18°, the upper breakdown emission phase Φ_u is 56°, and the impact energy $1/2\ mU_1^2 = 50$ eV. The trend of Hatch and Williams' experimental data is illustrated by the dashed curve of Fig. 2. The data for $80 < fd < 250$ MHz-cm were taken with silver-plated copper electrodes 3 centimeters apart.[3] For $fd > 250$ MHz-cm, the data were taken with outgassed aluminum electrodes at 140 MHz.[4] Hatch and Williams note that the exact shape of the curve for $fd > 250$ MHz-cm depends to a considerable extent on the condition (i.e., surface contamination) of the electrodes.

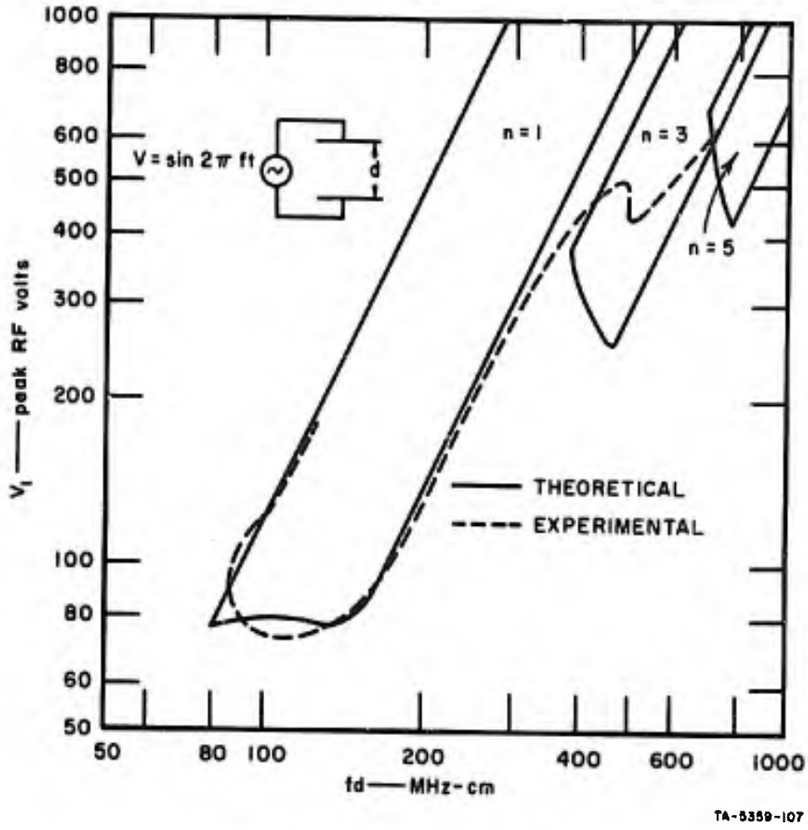

FIG. 2 MULTIPACTOR BREAKDOWN VOLTAGE AS A FUNCTION OF FREQUENCY AND GAP WIDTH FOR PARALLEL-PLANE ELECTRODES

B. Effect of Bias

If a dc voltage, in addition to the RF voltage, is applied to the multipactor discharge gap, the electron transit time will be shorter in one direction and longer in the opposite direction. The range of permissible electron-emission phase angles is sufficiently broad, however, that even with a moderate bias voltage on the gap, the electrons should be able to remain in synchronism with the RF field. The fact that multipactor discharges do occur in a biased gap has been demonstrated by a number of workers.[16-19] It has been demonstrated that in addition to the two-sided modes in which the electron crosses the gap and strikes the opposite electrode, there exists a one-sided mode in which the electron is carried away from the positive electrode by the RF field when the RF and dc fields are opposing, and driven back to the electrode from

which it was emitted during the next half-cycle when the RF field aids the dc field. The theory of multipactor discharge in a biased gap is limited to the case in which the electron emission energy can be neglected, however, except in the case of the one-sided modes. Simple theories neglecting the emission energy and the impact energy have been developed by Milazzo[18] and Zager and Tishin.[19] In the Zager and Tishin theory, the electron is required to make the round trip during one cycle, but no conditions are placed on the impact energy. In Milazzo's analysis, the electrons are required to make the round trip during an integer number of cycles and are required to strike the electrodes with a velocity greater than zero.

The region of multipactor discharge in a biased gap as determined from Milazzo's theory[18] for first-mode two-sided discharges and as determined by the authors' theory[16,17] for one-sided discharges is illustrated in Fig. 3, where the normalized RF voltage is plotted as a function of the normalized bias voltage along the contour of the breakdown threshold. The region of two-sided discharge is composed of a small region of stable discharge and a larger region of unstable discharge. At higher bias voltages, the region of stable one-sided discharge is encountered. Also of interest is the overlap of the one-sided and two-sided discharge regions at moderate bias voltages. The latter property of the biased discharge implies that the one-sided mode will generally be encountered before the two-sided mode is biased to cutoff. Note, however, that the minimum bias for the one-sided mode varies inversely with ωd; hence for very low frequencies or very small gap widths, the one-sided mode may not be observed at all.

Experimental data on multipactor discharge in a biased parallel-plate gap have been reported by the authors[17] and by Zager and Tishin.[19] The authors' data is shown in Fig. 4 for copper plates 15-cm in diameter and 5.25 cm apart at an RF frequency of 34.8 MHz. For convenience in comparing the experimental data with the theoretical results, the data are plotted in the normalized form and the region of two-sided discharge predicted by Milazzo's theory is shown. Also for comparison, the data of Hatch and Williams[3] at zero bias are shown.

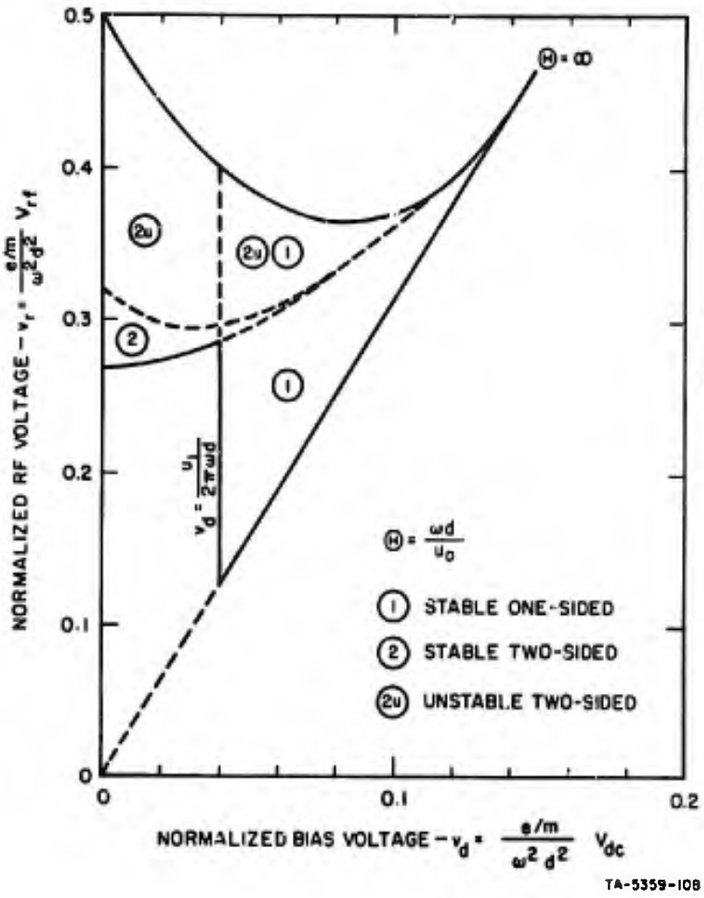

FIG. 3 BIASED MULTIPACTOR DISCHARGE REGIONS BASED ON SIMPLE THEORY

The interesting features of the experimental data of Fig. 4 are the size of region of multipactor discharge and the prominent region of one-sided discharge. The discharge region is m ch larger than that predicted by Milazzo for the stable and unstable regions combined. At least part of this difference between the experimental region and the predicted region is caused by neglect of the emission energy in the theory of biased discharges. At zero bias, for example, the inclusion of the emission energy can account for the lower RF threshold potential obtained experimentally by both the authors and Hatch and Williams. Other approximations in the theory undoubtedly contribute in a similar manner to the discrepancy between the experimental data and the predicted values.

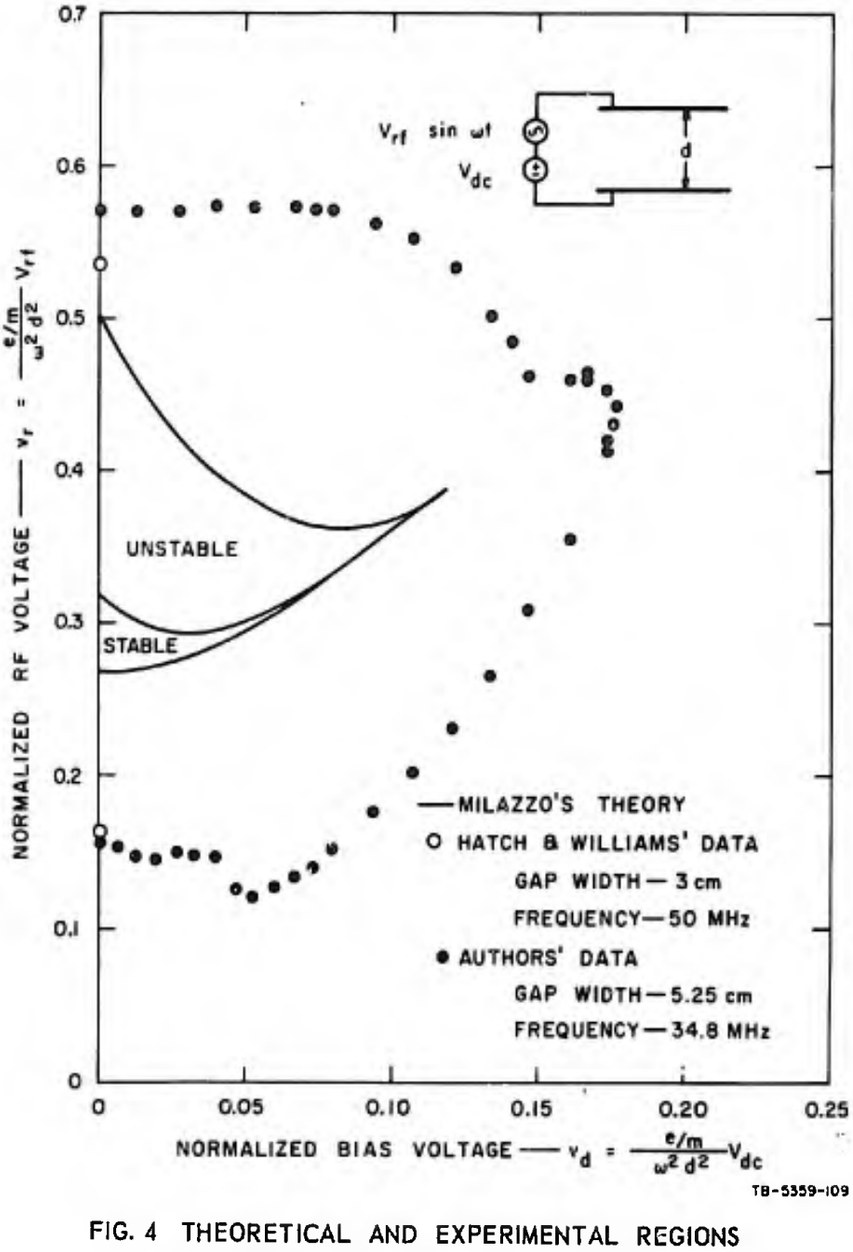

FIG. 4 THEORETICAL AND EXPERIMENTAL REGIONS OF BIASED MULTIPACTOR DISCHARGE

Zager and Tishin have published experimental data similar to that shown in Fig. 4 for values of fd ranging from 191 to 240 MHz-cm. These values are slightly higher than the 183 MHz-cm value of Fig. 5, but the Zager and Tishin data were taken with frequencies in the 9-to-23-MHz range with stainless steel electrodes. Their experimental data are

generally similar to those shown in Fig. 4 except that the upper RF breakdown threshold was somewhat lower. The upper and lower threshold potentials at zero bias and the cutoff bias voltages from the authors' data and from Zager and Tishin's data are tabulated in normalized form in Table I for comparison. [The actual voltages are multiplied by the normalizing factor $e/(m\omega^2d^2)$].

Table I

COMPARISON OF EXPERIMENTAL DATA

ON BIASED MULTIPACTOR DISCHARGE

Parameter	Authors' Data, Copper Electrodes, 34.8 MHz	Zager & Tishin's Data, Stainless Steel Electrode, 9-23 MHz		
fd (MHz-cm)	183	191	202	240
RF threshold (upper)	0.57	0.43	0.40	0.35
at zero bias (lower)	0.16	0.15	0.15	0.17
RF cutoff	0.44	0.33	0.34	0.31
Cutoff bias (dc)	0.176	0.16	0.17	0.17

The lower values obtained by Zager and Tishin for the upper RF breakdown threshold may be due to the difference in RF supply characteristics. The RF supply used by Zager and Tishin was a low-impedance source; thus the RF voltage applied to the electrodes was probably not affected much by the occurrence of the discharge. The RF sources used by the authors and by Hatch and Williams[8] contained high-Q resonant circuits that caused the electrode voltage to drop considerably when the discharge occurred. Since, according to Milazzo's theory, the upper threshold for the unstable discharge region is higher than the upper threshold for the stable region (see Figs. 3 and 4), it may be possible for the discharge initiated in the unstable region to load a high-impedance RF source sufficiently to lower the electrode voltage to the region of stable discharges where the discharge is sustained. With a smaller source impedance, however, the discharge would not be fully developed and sustained until the RF voltage was decreased to a level near the upper threshold for the stable discharge region. Abraham has observed a similar phenomenon which he attributed to initiation in the unstable region.[20]

The presence of the one-sided-discharge mode is evidenced in the lower breakdown contour of Fig. 4 by the sudden drop in the threshold voltage as the bias voltage increases. A similar discontinuity is observed in the upper breakdown contour. That the region to the right of these discontinuities is a region of one-sided discharge has been demonstrated experimentally in a parallel-plate electrode configuration in which only the one-sided mode could be sustained. By making one electrode of mesh coated with lamp black so that most of the incident electrons passed through the mesh and those that struck the wires of the mesh produced only a few secondaries (because of the lamp-black coating), it was possible to isolate the one-sided mode. Experimentally determined contours of one-sided multipactor discharge threshold are shown in Fig. 5 for two frequencies with copper electrode. Also shown in Fig. 5 are the theoretical contours of one-sided multipactor discharge.[16,17] These theoretical contours are defined in terms of the dimensionless parameters

$$\vartheta = \frac{\omega d}{U_0} \text{ and } k = \frac{U_1}{U_0}$$

where U_0 is the emission velocity of the electron and U_1 is the impact velocity required to produce a coefficient of secondary emission greater than one.

The practical importance of the one-sided discharge is two-fold. First, because the lower RF threshold for the one-sided mode is generally lower than the lower threshold for the two-sided modes for a given bias, the one-sided mode has the effect of lowering the threshold of RF breakdown. This effect is demonstrated in Fig. 3 where the theoretical breakdown curves for the one-sided and two-sided modes are compared, and in Fig. 4 where the experimental data show the reduction in RF threshold voltage as the bias is increased. Because of this property of the discharge, the use of dc bias to prevent multipactor discharges requires careful consideration, since insufficient bias, or partial failure of the bias system, can result in a lower RF breakdown voltage than would obtain in the absence of bias.

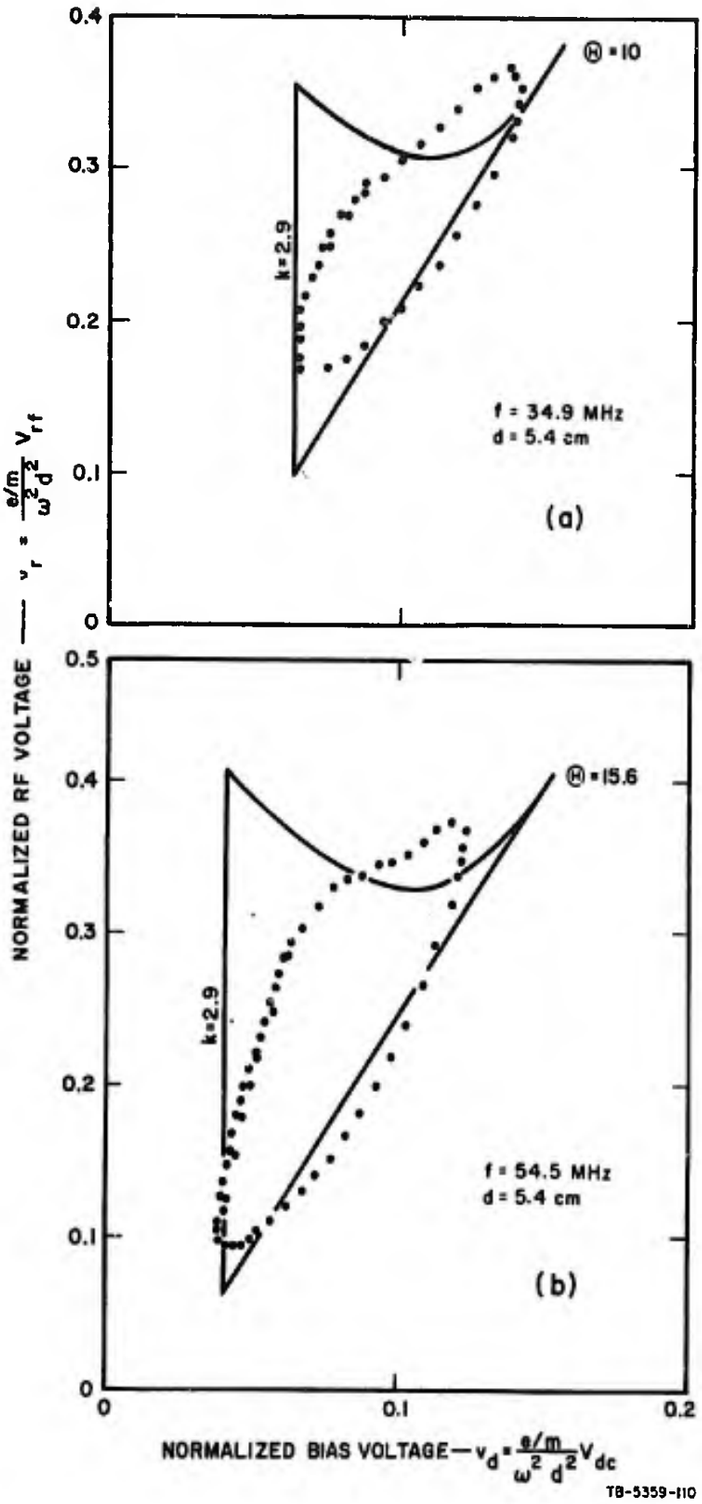

FIG. 5 EXPERIMENTAL THRESHOLD CONTOUR WITH CLOSEST-FITTING THEORETICAL CONTOUR SUPERIMPOSED

The second property of the one-sided discharge that is of practical concern is its effect on circuit elements. Because the one-sided discharge is predominantly reactive (in the uniform field case), the reactive loading associated with the discharge can detune resonant RF circuits, thereby seriously degrading the performance of the RF system. Although the discharge should be purely reactive in a uniform field during buildup, space-charge effects probably distort the field sufficiently that the developed discharge absorbs RF power as well as dc power. The developed discharge would thus have resistive, as well as reactive, components of impedance.

In addition, it has been observed in experiments with biased multipactor discharges that a discharge often initiates in the one-sided mode, and in high-impedance circuits rapidly makes a transition to the two-sided mode. If, for example, a large series resistance is used in the bias circuit to protect the bias supply, the bias voltage at the electrodes may drop sufficiently, when the one-sided mode is initiated (and the gap becomes conductive), that a strong two-sided mode is accommodated. (If a current-limiting resistor is not placed in series with the power supply, damage to the power supply or other components may be incurred because of scintillation discharges. This phenomenon is discussed in more detail in Sec. III.)

C. Effect of Electrode Materials

Because the multipactor discharge is dependent on secondary emission of electrons from the electrodes to produce the free charge in the sustained discharge, the characteristics of the discharge are relatively independent of the residual gas in the discharge region, but they might be expected to depend considerably on the electrode materials. Surprisingly, however, there appears to be very little difference in the performance of many of the common metals as electrodes. Commercial grades of copper, brass, aluminum, and steel display very minor differences in threshold potentials for multipactor discharges; the differences between materials are comparable to the differences that are observed with the same material under different conditions of surface contamination,

outgassing, etc. Some of the materials that have been tested as multipactor electrodes are indicated in Table II.

Table II

MULTIPACTOR PROPERTY OF ELECTRODE MATERIALS

(x supports multipacting; 0 does not support multipacting)

Electrode Material	Gill & Von Engel[6]	Hatch & Williams[4]	Krebs & Meerbach[11]	Vance & Nanevicz	Zager & Tishin[19]
Metals					
Copper		x	x	x	x
Aluminum		x	x	x	x
Iron (low-carbon steel)			x	x	x
Stainless steel					x
Titanium				0	x
Silver (and silver plate)		x	x	x	
Gold plate				x	
Brass				x	
Insulators					
Teflon				x	
Soft glass	x				
Hard glass	x				
Coatings					
Lamp black				0	
Palladium black	0			0	

It is noted that multipacting is supported by all of the metals and insulators listed in Table II, with the possible exception of titanium. Zager and Tishin indicate that the titanium electrodes they used supported multipactor discharges about as well as other metals, but no account is given of the type of titanium or the extent of the tests conducted with titanium. The authors performed a very brief test using

Ti70A titanium sheet for electrodes and found that it did not support multipactor discharges. In addition, Preist has conducted extensive experiments in high-power microwave devices in which he has used titanium films to eliminate multipactor discharges.[21,22] It is suspected that the behavior of titanium as a multipactor electrode material depends to a considerable extent on the purity of the titanium. According to the published data on secondary emission yield, the maximum coefficient of secondary emission, δ_{max}, is less than unity (i.e., one gets less than one secondary electron for each primary) for pure titanium. Thus if pure titanium electrodes were used, electron multiplication could not occur. However some commercial alloys, or pure titanium with a contaminated surface, might support the discharge. The Ti70A sheet used by the authors is a commercially pure titanium.

The maximum secondary emission coefficients δ_{max} and the energy of the incident electrons V_{pmax} (in electron volts) at which δ_{max} occurs is shown in Table III for a number of elements. As can be seen, most of the metals commonly used in aerospace structures have maximum secondary emission coefficients greater than unity. It is not surprising, therefore, that most metal electrodes will support multipactor discharges. The prominent exceptions that have secondary emission coefficients less than unity are titanium, magnesium, and beryllium. These metals are often used in an alloyed form, however, and the alloy often has a higher secondary emission yield than the pure metal. Forrer and Milazzo,[23] for example, indicate that a silver-magnesium alloy was chosen for the electrode material in their microwave switch because of the copious secondary emission produced by this material. In addition, on metals such as magnesium, an oxide film is readily formed on any surface exposed to the air. The secondary emission yield of the oxide is much greater than the yield of the base metal.

Because surface films do form on most metals (including the noble metals) it is perhaps more appropriate to consider the secondary emission yield of the metal compounds. Table IV shows the values of δ_{max} and V_{pmax} and the values of V_p^I and V_p^{II} at which δ is unity. It is important to multipactor discharge theory that the oxides and halides have much greater secondary

Table III

MAXIMUM SECONDARY ELECTRON EMISSION YIELD δ_{max}, AND CORRESPONDING V_{pmax}, FOR DIFFERENT ELEMENTS*

Element	δ_{max}	V_{pmax} (Volts)
Ag	1.5	800
Al	1.0	300
Au	1.46	750
B	1.2	150
Ba	0.83	400
Bi	1.15	550
Be	0.53	200
C	1.0	300
Cd	1.1	400
Co	1.2	700
Cs	0.72	400
Cu	1.3	600
Fe	1.3	350
Ge	1.2	400
K	0.75	200
Li	0.5	85
Mg	0.95	300
Mo	1.25	375
Nb	1.2	375
Ni	1.3	550
Pb	1.1	500
Pd	>1.3†	>250†
Pt	1.8	800
Rb	0.9	350
Si	1.1	250
Sn	1.35	500
Ti	0.9	280
W	1.4	700
Zr	1.1	350

*Source: Ref. 24

†$\delta = 1.3$ at $V_p = 250$ V is not maximum value of δ.

Table IV

MAXIMUM ELECTRON YIELDS FROM SOME METAL COMPOUNDS*

	δ_{max}	V_{pmax} (Volts)	V_p^I (Volts)	V_p^{II} (Volts)
LiF	5.6		21	
NaF	5.7		20	
NaCl	6.8 to 6	600	15	
KCl	7.5		15	
RbCl	5.8			
CsCl	6.5			
NaBr	5.5			
KI	5.5		12	
Cs_2O†	2.3 to 11			
$SbCs_3$	5 to 8.3	375 450	10 20	
CaF_2	3.2			
BaF_2	4.5			
BeO	3.4	2000		
MgO	2.4 to 4.0	1500 to 400		
BaO	2.3 to 4.8	1600 to 400		
CaO	2.2	500		
Al_2O_3	1.5 to 4.8	350 to 1300		
mica	2.4	380	30	3300
SiO_2 (quartz)**	2.1 to 2.9	400 to 440	30 50	 2300
Ag_2O	0.98 to 1.18			
MoS_2	1.10			
MoO_2	1.09 to 1.33			
WS_2	0.96 to 1.04			
Cu_2O	1.19 to 1.25			

*Source: Ref. 24

†The values of δ_{max} in the table are the highest obtained as of (1953)

**Glasses mostly show a secondary emission yield of the same order of magnitude as quartz.

emission yield than the base metals. Thus, for example, aluminum, which has a δ_{max} of 1.0 should barely support multipactor discharges if all electron loss mechanisms were eliminated, but Al_2O_3, which always forms on the surface of aluminum worked in the atmosphere, has a δ_{max} of 1.5 to 4.8; hence aluminum electrodes usually support multipactor discharges quite well. Note in Table IV also that the values of V_p^I (the impact energy at which δ first exceeds 1.0) for many of the compounds lie in the range between 10 and 30 eV. Since the most probable energy of the secondary electrons is about 5 volts, the values of k, which have been observed to be in the vicinity of 3 or 4 in multipactor experiments, appear to be consistent with the assumption of a contaminated surface rather than a pure metal surface.

Multipactor discharges on dielectric surfaces produce some interesting effects if dc bias is applied with the RF field. These effects were observed in the laboratory by placing thin Teflon sheets over the surface of the 6-inch-diameter parallel discs used for multipactor electrodes in the laboratory. The electrodes were driven with a signal generator through a tuned, balanced circuit similar to the unbalanced circuit used in the coaxial tests described in Sec. III. Without bias, the multipactor discharge occurred from the Teflon surfaces at approximately the same RF voltage and with approximately the same intensity as from metal electrodes. When bias was applied prior to applying the RF voltage, the breakdown characteristics were again similar to those obtained with metal electrodes--that is, application of moderate bias caused a slight reduction in the lower RF threshold, and application of a strong bias would prevent the discharge from starting.

If the gap were not biased beyond cutoff, however, and a discharge was produced and allowed to extinguish without changing the bias, the effect of the bias would be eliminated. Therefore, if the bias supply voltage were not changed, the gap would behave as though it were not biased. The explanation of this behavior lies in the fact that when the discharge occurs in a biased gap with insulated electrodes, the gap becomes conductive and the bias field drives charge to the insulating

surface of the electrodes until the bias field in the gap is zero. Thus all of the bias voltage is dropped across the insulation layer, and none remains across the gap. On good insulators the charge trapped on the surface will remain for long periods of time, and if the bias source voltage is not changed, the bias field in the gap will remain near zero long after the discharge has been extinguished. On the other hand, if the bias source voltage is reduced to zero after the discharge is extinguished, the charge trapped on the insulating surface will cause a reverse bias in the gap.

Note that the application of bias to the gap with insulated electrodes effects only the starting potential of the discharge. Once the discharge has started, the gap becomes conductive and nullifies the static field in the gap regardless of what bias potential is applied to the electrodes behind the insulation. It is possible, therefore, to increase the bias potential to beyond that normally required for cutoff, after the discharge has started, without affecting the discharge, since changing the bias then only changes the charge deposited on the surface of the insulation. If the bias source voltage is beyond the cutoff value when the discharge extinguishes, and is reduced to zero after the extinction, the charge trapped on the surface insulation will bias the gap to cutoff with no source voltage.

While many of these observations fall in the category of laboratory curiosities, they also have some practical implications. For example, as a consequence of this behavior, one would not attempt to prevent multipactor discharges in an insulated gap by applying a static bias, since the effectiveness of the bias can be destroyed by a single burst of ionization in a fraction of a second, or, over a period of seconds or minutes, by the acquisition of surface charge from ambient ionization in space.

BLANK PAGE

III MULTIPACTOR DISCHARGE IN A COAXIAL GEOMETRY

A. Threshold Potentials

The possibility of the multipactor discharge occurring in a coaxial geometry has important implications for designers of RF components on spacecraft. Bol made a cursory analysis of multipactor discharge conditions in a coaxial geometry and concluded that under certain assumptions and conditions the discharge would be possible.[25] In the same article, however, Bol states that "...multipactor unrestrained by a magnetic field simply does not occur unless the actual geometry closely resembles the parallel plane case." Since Bol's paper left some doubt as to whether or not the discharge does occur in a coaxial geometry, an experiment to investigate this phenomenon was arranged. Because some interesting side effects had already been observed as a result of applying a bias to parallel-plane electrodes, provision was also made to bias the coaxial electrodes.

The mechanical construction of the coaxial electrodes used for these experiments is shown in Fig. 6. A 3-inch-ID copper tube was used for the outer conductor, and smaller tubes or wires were used for the inner conductor. To minimize the possibility of discharges occurring in the vicinity of the feed point, a baffle was placed around the RF feed area so that all gaps in this area were too short to support multipactor discharges. This baffle structure was also coated with lamp black to further reduce the possibility of discharges originating in this area. The end opposite the feed point was left open so that the discharge in the structure could be observed through the wall of the bell jar vacuum chamber.

A schematic of the RF and biasing circuit used in these experiments is shown in Fig. 7. The RF voltage supplied to the coaxial geometry was provided by a tuned circuit driven by a signal generator. A dc blocking capacitor provided static isolation of the center conductor from the outer conductor of the coaxial electrodes. The dc bias voltage was

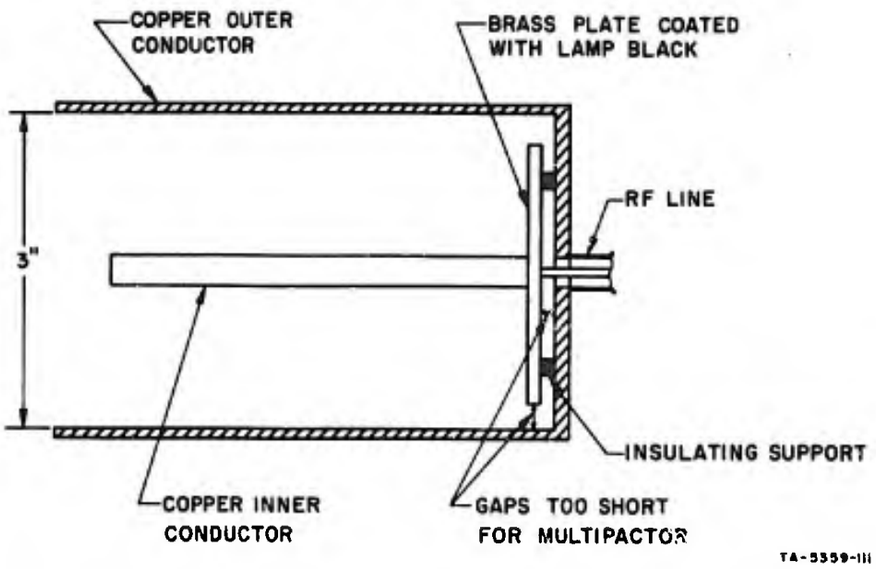

FIG. 6 COAXIAL ELECTRODE STRUCTURE USED FOR MULTIPACTOR THRESHOLD TESTS

applied across this capacitor through a 1-MΩ resistor. A loosely coupled RF metering circuit was used to measure the RF voltage applied to the electrodes. A microameter in the dc bias circuit afforded a convenient means of detecting the onset of the discharge, since as soon as the discharge occurred, the coaxial gap became slightly conductive and a small current could be detected in the bias circuit.

The coaxial electrodes were commercial copper cleaned by scrubbing with a commercial abrasive cleanser prior to each test run. The electrodes were not baked out or degassed; they were scrubbed and placed in the bell jar and pumped down to approximately 10^{-4} torr for about 30 minutes before the test run. Some outgassing was undoubtedly associated with the preliminary discharges that were produced in the process of tuning and testing the RF system; however, there was no deliberate effort to outgas the electrodes.

Measurements of RF breakdown threshold voltages were made at 38 MHz for center conductor diameters ranging from 0.031 to 0.50 inch. Since the inside diameter of the outer electrode was 3.0 inches the ratio of outer to inner conductor diameter ranged from 6 to 97. Data from these

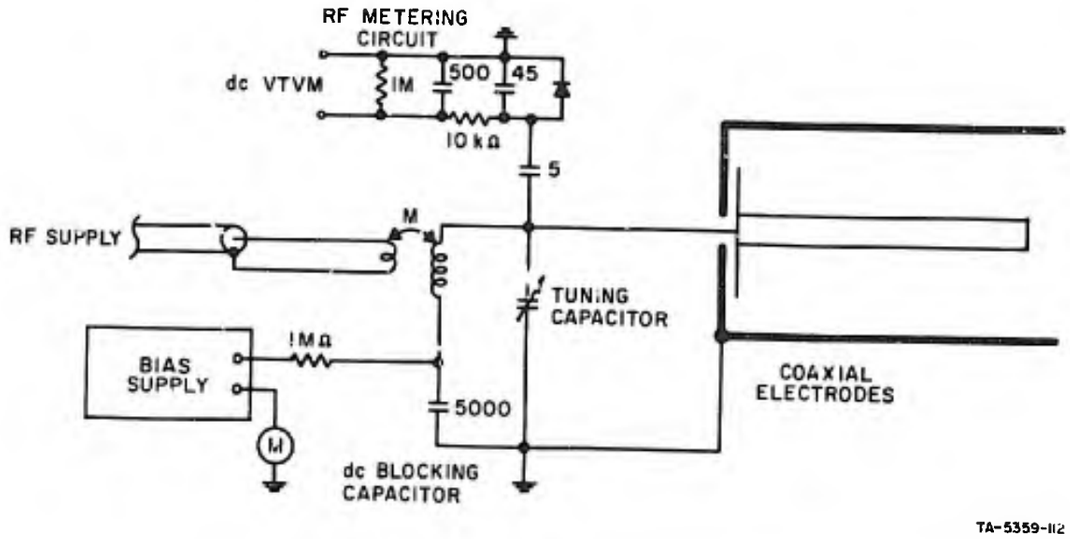

FIG. 7 CIRCUIT FOR TEST IN COAXIAL GEOMETRY

measurements are plotted in Fig. 8 for the five inner-conductor diameters. Data for the lower RF threshold were obtained by setting the dc bias and increasing the RF voltage until breakdown occurred. To obtain the upper threshold, the electrodes were biased beyond cutoff, and the RF voltage was increased to above the threshold. The bias was then reduced to the desired level, and the RF voltage was reduced until breakdown occurred. The most reliable indication of breakdown was the step increase in the bias current that occurred when the increased electron density between the electrodes made the gap conductive. This increase in bias current (or drop in bias voltage as a result of current through the 1-MΩ resistor in the bias circuit) could be easily detected even when the discharge was so weak that it was difficult to see or so weak that it did not produce a drastic drop in the RF voltage by detuning the high-impedance RF tank circuit. (These very weak discharges appeared to be associated with the discharges occurring at large bias voltages where the discharge was apparently occurring as a weak one-sided discharge.)

An interesting feature of the data of Fig. 7 is that the region of RF and bias voltages over which the discharge occurs increases as the center-conductor diameter is reduced. It appears that the increase in the size of the discharge region is due to the formation of a larger

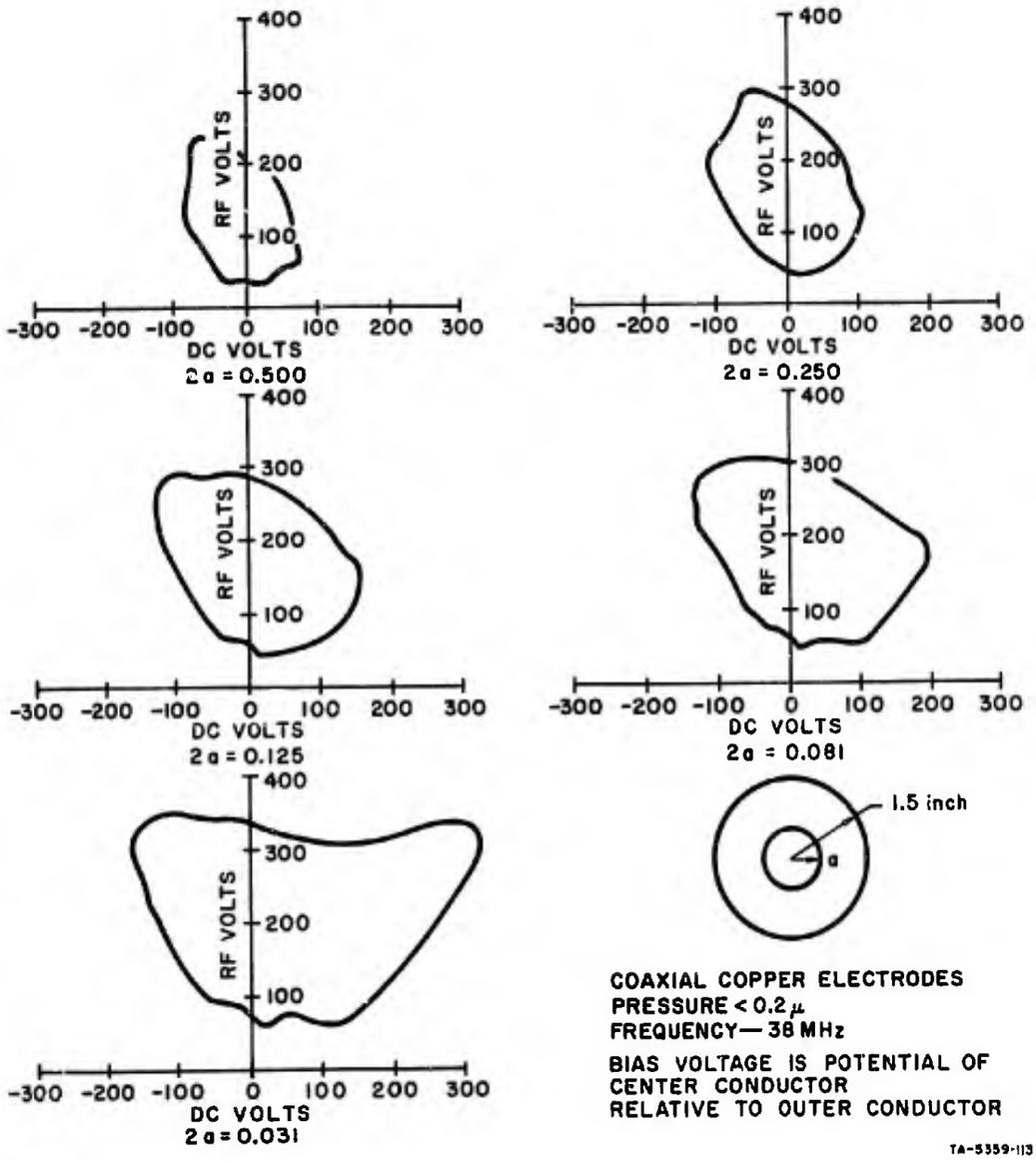

FIG. 8 REGIONS OF MULTIPACTOR DISCHARGE IN A COAXIAL GEOMETRY

region over which the one-sided discharge mode can operate. The shapes of the contours shown in Fig. 8 (particularly those for the smaller center conductors) are reminiscent of the contours obtained in the biased parallel-plate gap where the potato-shaped region of the one-sided discharge is merged into the region of the two-sided mode.

Also of interest is the fact that at the larger positive bias values, the RF threshold for multipactor discharge is lower than the dc bias

voltage. The RF voltages in Fig. 8 are rms values, but even when they are converted to peak-voltage values, the RF voltage is less than the dc bias voltage for a significant portion of the lower breakdown curves for the three smallest center conductors. In each case, however, this phenomenon occurs in a region that appears to be a one-sided multipactor discharge region. The analysis of the discharge in a coaxial geometry is complicated because of the non-linear differential equation for electron motion; however, a feeling for the problem can be obtained by considering the case of a square-wave RF voltage. If the amplitude of the square wave voltage is less than the bias voltage by just the electron emission energy (in electron volts), an electron emitted at the center conductor has just enough energy to reach the outer electrode, provided that the electron is emitted when the RF field opposes the dc field and that the RF field remains in opposition to the dc field for the duration of the electron transit. Suppose, in addition, that the field reverses just as the electron reaches the end of its transit, but before it strikes the electrode. Then the RF field is aiding the dc field in forcing the electron back toward the electrode from which it was emitted. If the electron can make the transit back to the electrode within one-half period, it will have acquired an energy equal to the sum of the peak RF voltage and the bias voltage.

Suppose now that the RF amplitude is less than the dc bias voltage by more than the emission energy. Then the electron will be stopped before it quite reaches the outer electrode; however, since it may not be stopped until it reaches the lower field region away from the center conductor, it will not be strongly accelerated back toward the center conductor until the RF field reverses. Thus, a one-sided mode would be possible even though the RF amplitude were significantly less than the bias voltage.

Because the electron motion must remain approximately synchronous with the RF field, discharges in which the RF voltage is less than the dc voltage can only occur in non-uniform fields such as those of the coaxial geometry. In the coaxial geometry, the returning electron ex-

periences the strongest acceleration immediately before impact. Hence, the transit time back to the electrode when the fields are aiding is of the order of the transit time away from the electrode when the fields are in opposition. In the uniform-field case, however, the transit time back to the emitting electrode is much less than the transit time away from the electrode, and the electron motion cannot be made synchronous with the RF field (if the dc field exceeds the RF field). With a sinusoidal RF voltage, the allowable excess of bias voltage over peak RF voltage will be somewhat less than for the square-wave. On the other hand, the requirements for synchronous electron motion are less stringent for the sine-wave case because the fields change more gradually from the opposing condition to the aiding condition.

The diameter ratios tested are somewhat larger than those encountered in RF coaxial transmission lines except perhaps in transitions from solid dielectric lines to air-dielectric lines. Typical diameter ratios for air-line and solid dielectric ($\epsilon_r = 2$) line are shown in Table V. The

Table V

TYPICAL DIAMETER RATIOS FOR
COAXIAL TRANSMISSION LINE

Characteristic Impedance (ohms)	Diameter Ratio	
	Air Dielectric	Solid Dielectric ($\epsilon_r = 2$)
50	2.3	3.2
75	3.5	5.9
93	4.7	8.9

largest center conductor tested corresponds to an air-line impedance of 108 Ω. It is noted, however, that the behavior of electrodes with smaller diameter-ratios approaches the behavior of the parallel-plate electrodes. This is confirmed by Woo's data for a diameter ratio of 2.3.[26] Hence multipactor breakdown in very low-impedance lines should be similar to breakdown between parallel plates.

B. Power Dissipated in Discharge

The information presented so far has been concerned with the threshold voltages for multipactor breakdown. This information answers the question, "when does multipactor breakdown occur?" The next question the designer wishes to answer is, "what happens when multipactor breakdown occurs?" One of the primary concerns will be the power dissipated in the discharge and the manner in which it is dissipated. In this section, the results of some attempts to measure the power dissipated in a discharge will be described.

Power measurements were made in three copper coaxial lines at frequencies in the 230-to-260-MHz range. The most extensive measurements were made in a structure having a 2-inch-diameter outer conductor and a 1.63-inch-diameter inner conductor, as shown in Fig. 9. Holes 1/4 inch in diameter were drilled through the outer conductor at several points along the line to allow the space between the coaxial conductors to be freely vented, and to allow the glow from the discharge to be seen. A small pill-box was installed over one of the holes to capture the multipactor electrons incident on the outer conductor. The electron current to the pill-box was measured with a D'Arsonval meter enclosed in a shield covering the pill box.

The coaxial test structure was driven with a 230-MHz moderate-power ($\leq$200 watts) transmitter with provisions to monitor the incident power, reflected power, and power transferred to a load on the other side of the test section. The RF circuit showing placement of the transmitter, directional couplers, test section, and power meters is shown in Fig. 10. Because the test section was designed to have nearly uniform fields in the coaxial gap and the ends were designed to prevent discharges, the test section did not match with the 50-Ω RF supply source. The line was one-quarter wavelength with Z_0 approximately 14 Ω, and each end had about 20 pf of capacitance. A variable capacitor was placed in parallel at each end of the coax; in order to match the generator to the load. It was found that the optimum settings for breakdown did not quite coincide with an optimum match. It was found, however, that the match improved after breakdown occurred (see Fig. 14).

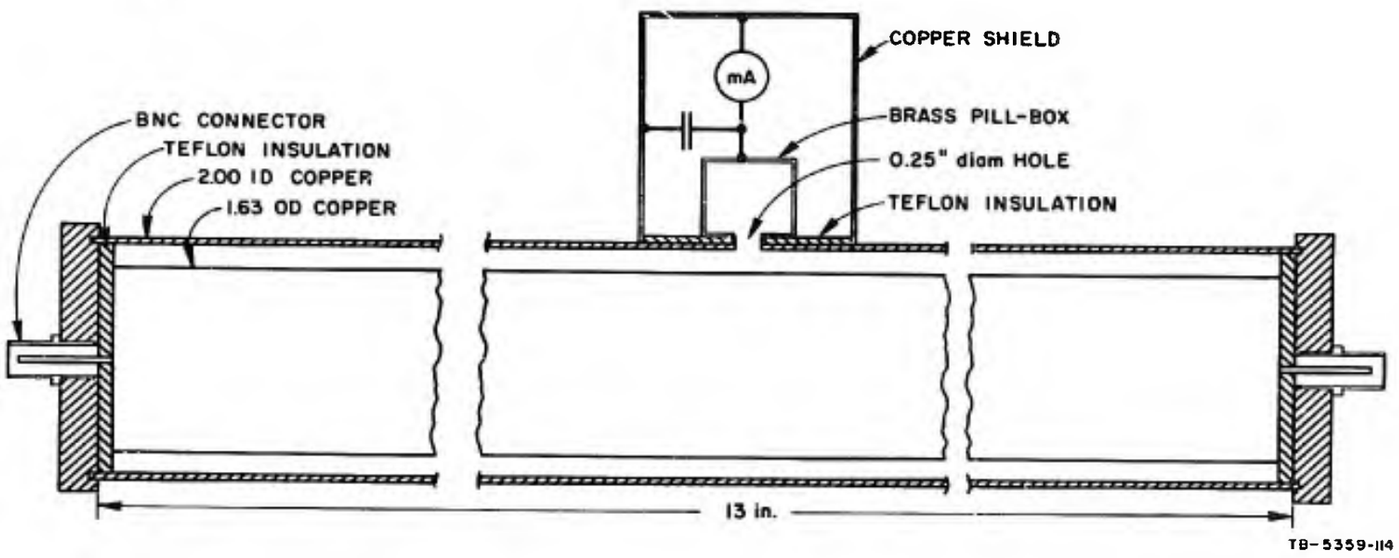

FIG. 9 ELECTRODE STRUCTURE FOR MULTIPACTOR POWER MEASUREMENTS

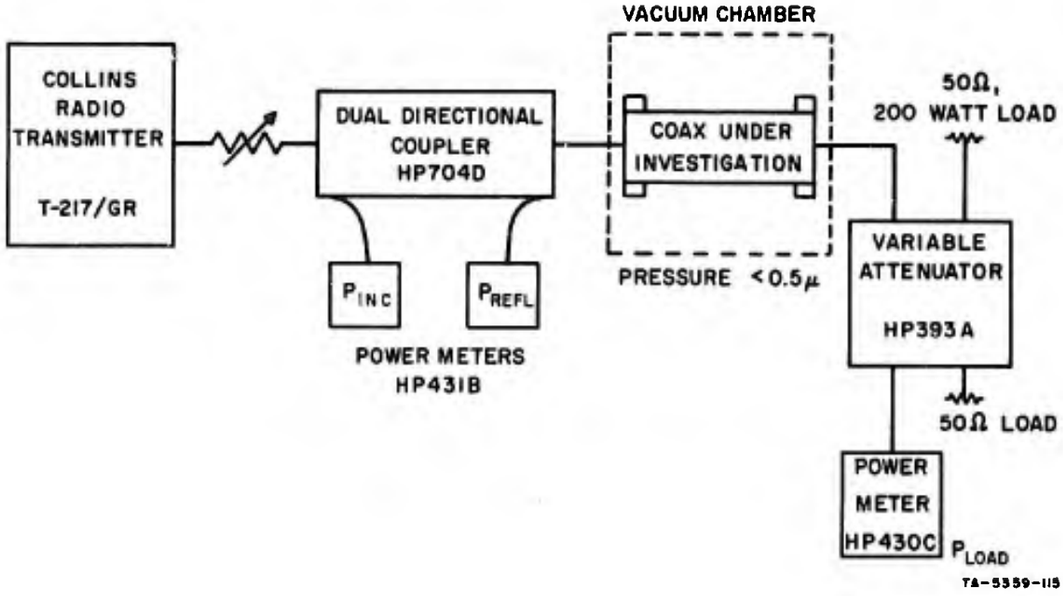

FIG. 10 RF CIRCUIT ARRANGEMENT FOR POWER MEASUREMENTS

To measure the power absorbed by the discharge, we plot the power to the load P_{load}, against the power delivered to the network, $P_{inc} - P_{refl}$. We find that the slope drops off after breakdown occurs, and by extrapolating the initial slope, we may determine approximately how much power is absorbed. Typical data are shown in Figs. 11 and 12 for the test structure of Fig. 8 at 230 MHz. Breakdown occurred during these tests with about 55 watts delivered to the test section, and thereafter, part of the power delivered to the section was absorbed by the multipactor discharge. For comparison, a third set of data was taken at atmospheric pressure to verify the linearity of the power meters and other components at the power levels above 50 watts. These data are shown in Fig. 13. The trial at atmospheric pressure indicates that P_{load} is linear when breakdown does not occur. However, it may be possible that the power lost in the RF circuits is altered by breakdown. The reflection coefficient is changed by the discharge, and in this case it tended to bring about a better match. In Fig. 14, reflected power is plotted against incident power for the same three data sets shown in Figs. 10, 11, and 12. Because the match improved when the discharge

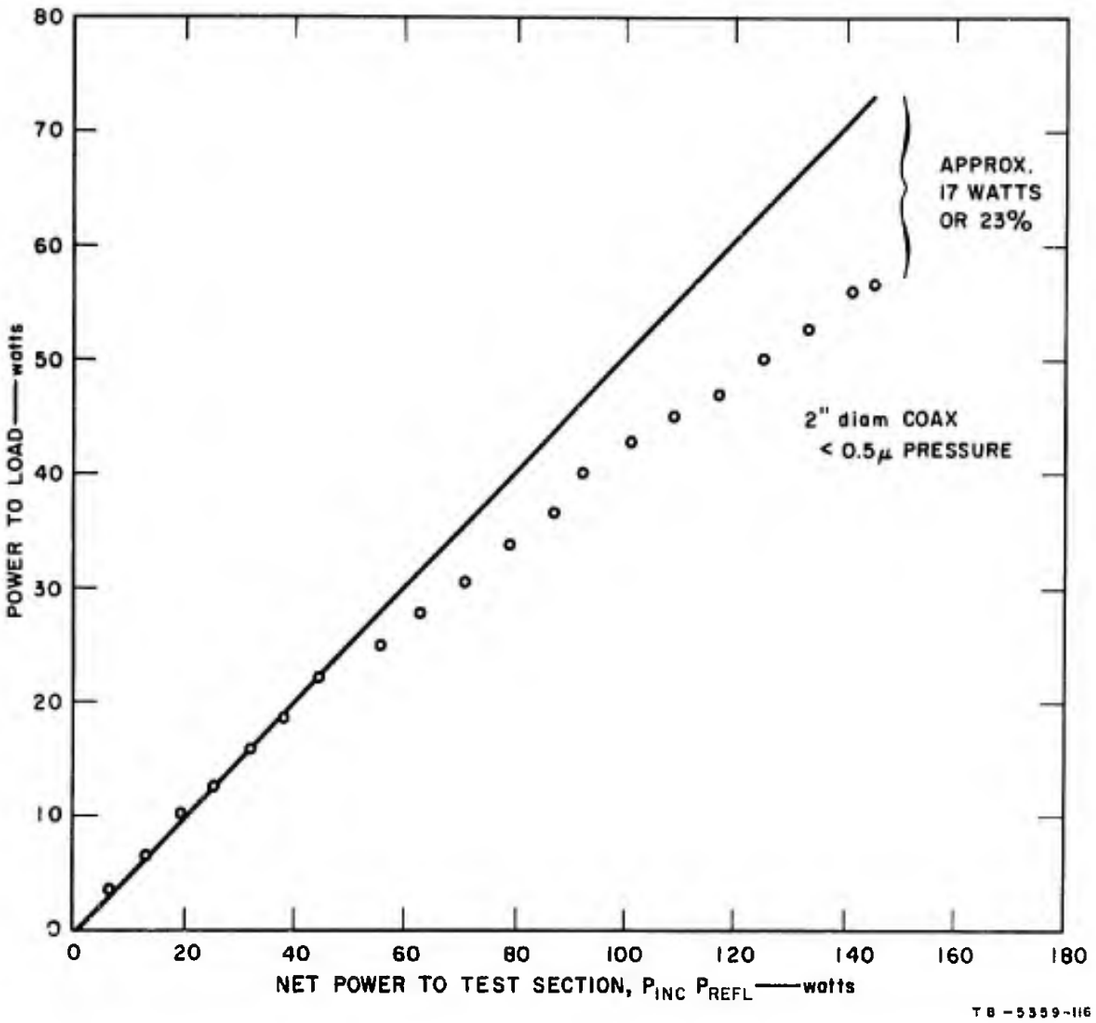

FIG. 11 TRANSMITTED POWER AS A FUNCTION OF NET POWER TO TEST SECTION

occurred, however, it is anticipated that any correction that might be necessary as a result of the SWR change would result in an increase in the power apparently absorbed by the discharge.

After several tests, the pill-box shown in Fig. 9 was installed over one of the 1/4-inch-diameter vent holes in the outer conductor to measure the electron current passing through this hole. (Observations of the discharge through these holes during the earlier tests indicated that there was a standing wave in the test structure; the brightness of the discharge varied along the length of the structure.) The pill box

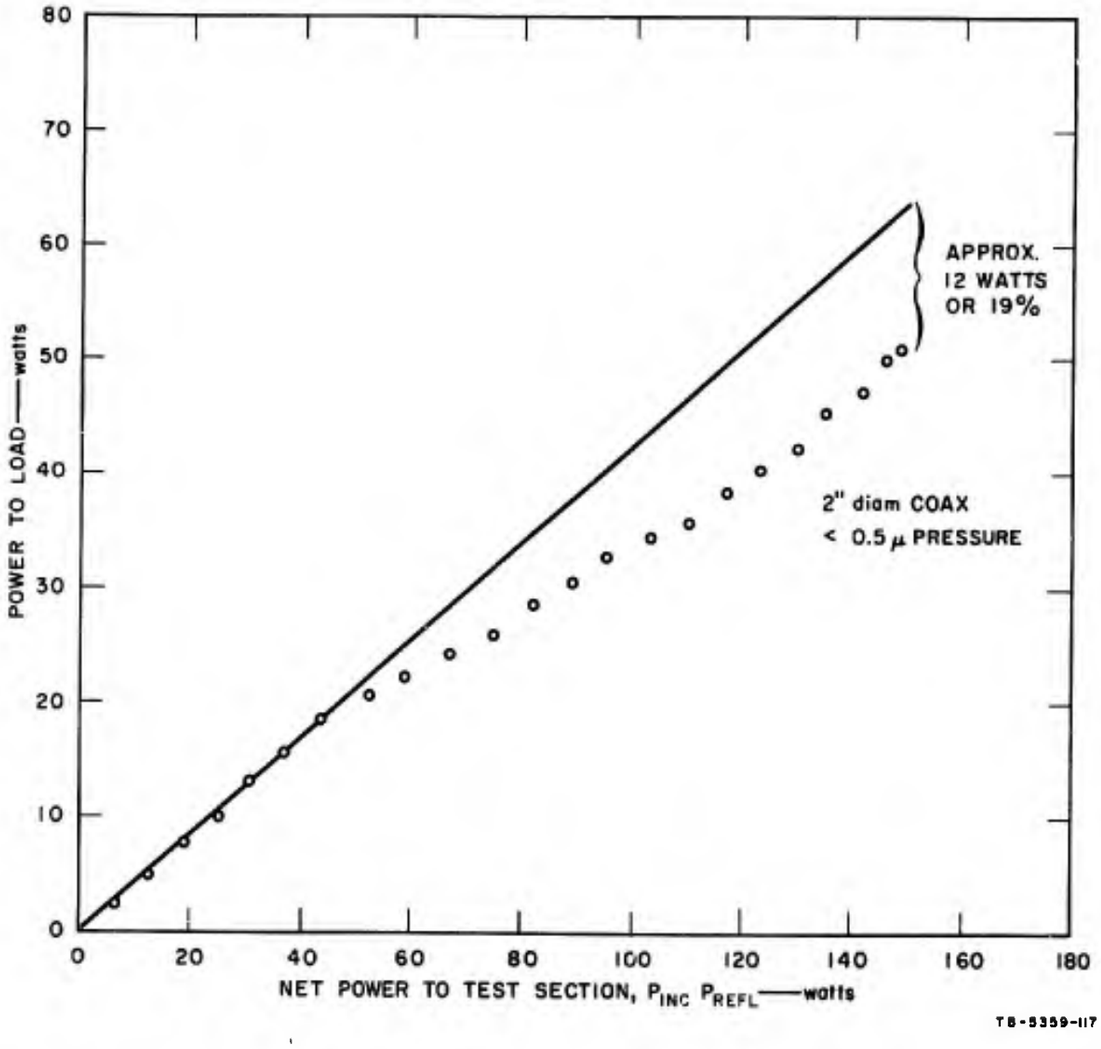

FIG. 12 TRANSMITTED POWER AS A FUNCTION OF NET POWER TO TEST SECTION

was installed over one of the holes where the discharge appeared to be brightest. A maximum current to the pill box of approximately 0.1 mA was observed.

Let us assume an electron density of n electrons per square meter in the electron "sheet" that is driven back and forth across the gap during the multipactor discharge. Then, neglecting fringing, the current through the hole to the pill-box would be

$$I = nfe\ A$$

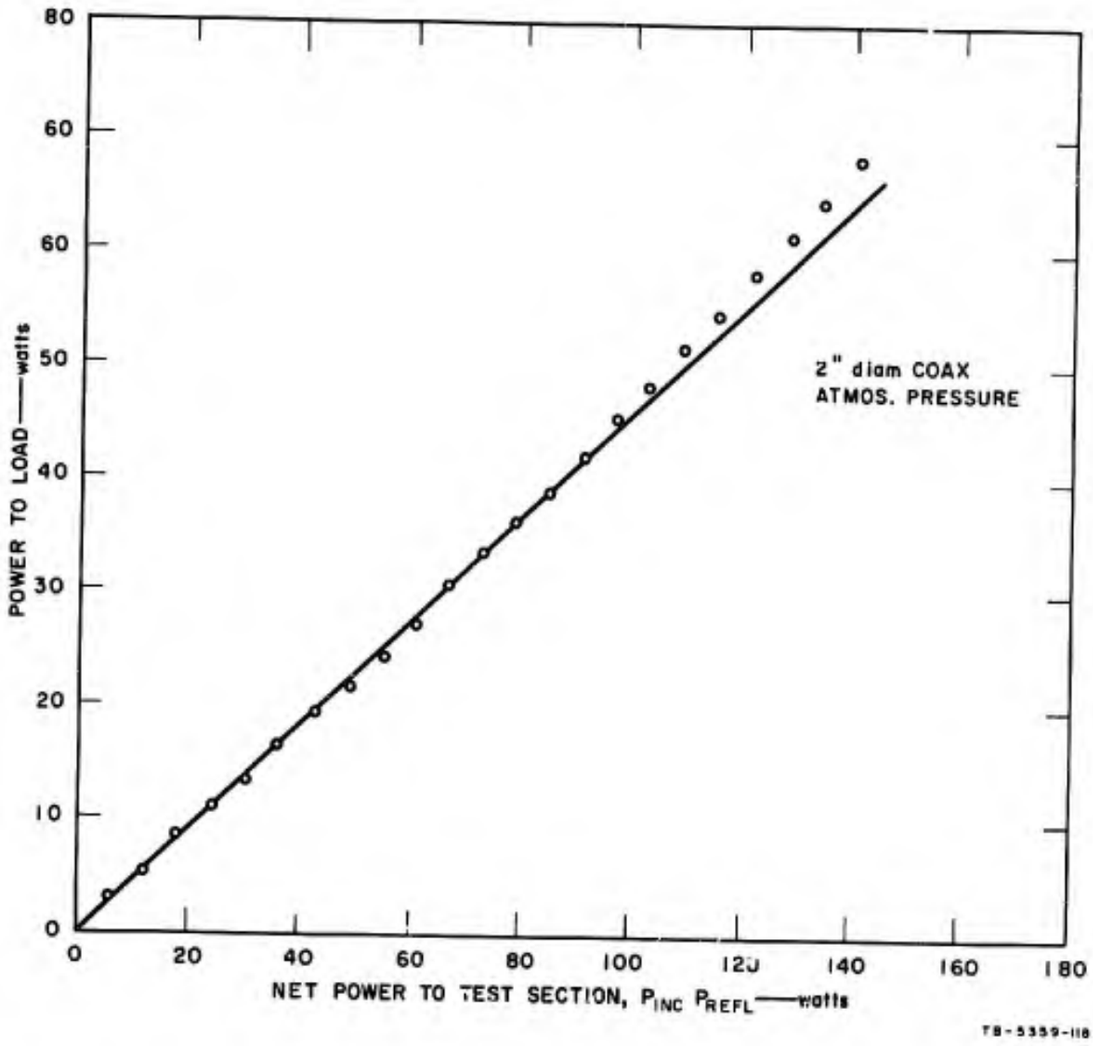

FIG. 13 POWER METER PERFORMANCE IN ABSENCE OF BREAKDOWN

where A is area of the hole, f is the RF frequency, and e is the charge on the electron. Solving for n, we have

$$n = \frac{I}{efA}$$

$$= 1.5 \times 10^{11} \text{ electrons/m}^2$$

for the 0.1-mA current through the 1/4-inch-diameter hole. If this electron density were uniform over the test structure, the total number

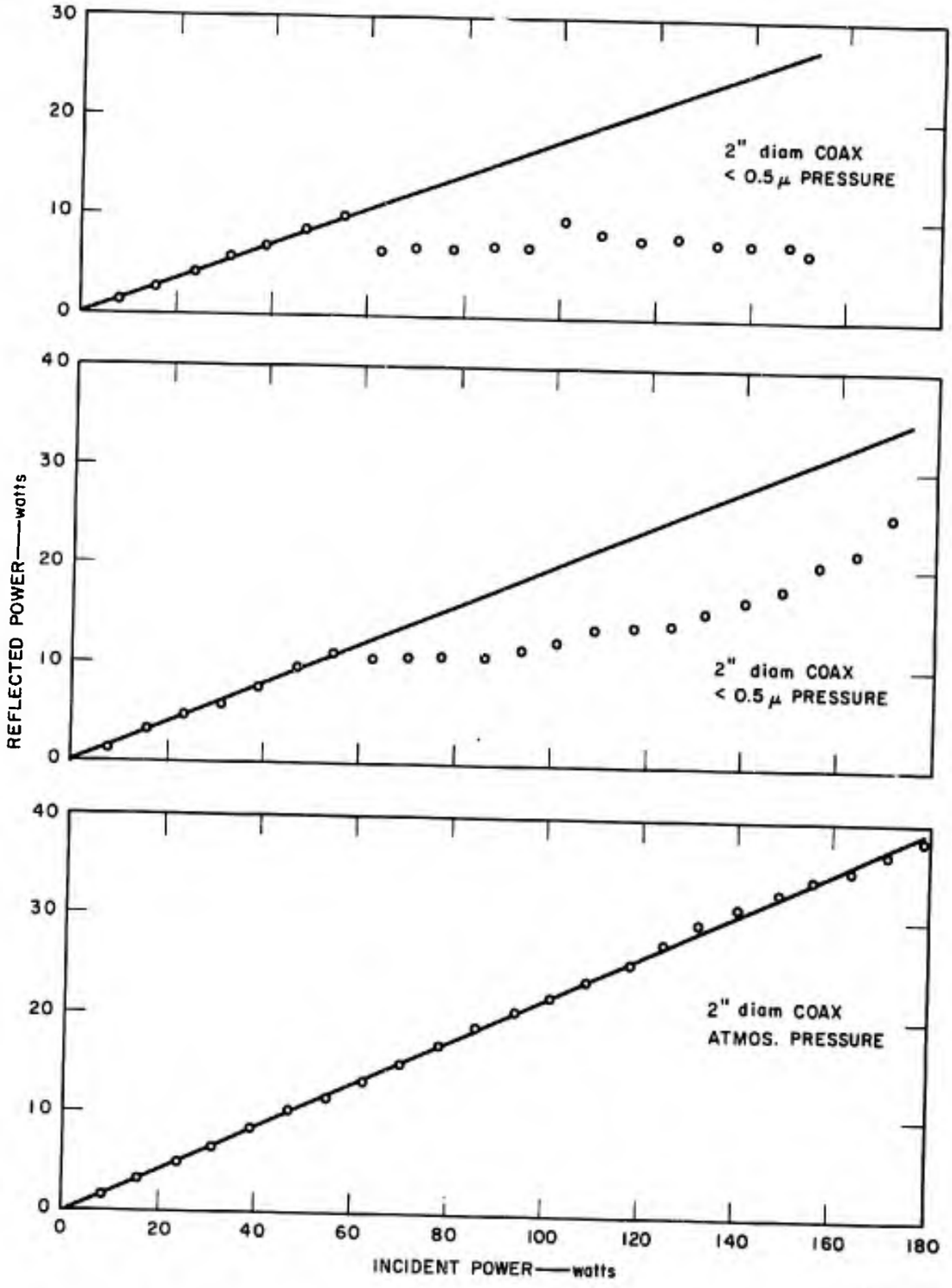

FIG. 14 REFLECTED POWER VARIATION WITH INCIDENT POWER, WITH AND WITHOUT BREAKDOWN

of electrons participating in the discharge would be 7×10^9 electrons. Reference 23 indicates that approximately 10^{10} electrons participated in a discharge at 3 GHz, covering perhaps 1/10 the area of the coaxial gap used here.

The power dissipated in the discharge is

$$P = 2eV\ nf\ A$$

since there are nA electrons crossing the gap 2f times per second and giving up eV joules of energy each on striking the electrodes. For 100 watts through the 14-ohm electrode geometry, the peak RF voltage is 53 volts. Hence, if it is assumed that the electron energy is of the order of the peak RF voltage, the power dissipated in the discharge would be 27 watts. This is of the order of (but somewhat larger than) the apparent power loss indicated on Figs. 10 and 11.

In order to further verify that the power loss is a result of the discharge and not of the matching network, the experiment was repeated with an 18-inch length of coax, which closely approximated a 50-ohm line. The outer conductor was approximately 1-inch in diameter, and the inner approximately 0.45 inch. Data from this experiment are shown in Figs. 15 and 16, where the 243-MHz transmitted power is again plotted against the net power into the test section. Less power was dissipated in the discharge in this test section, but the area of the discharge was smaller and the geometry was more non-uniform.

Additional experiments were conducted with Type N and GR-874 coaxial connectors. A small hole was drilled through the outer conductors of these connectors to vent the air out of the interior. The tests on these connectors were performed in the same manner as the earlier tests on the special coaxial sections. No power loss could be detected in either connector, but a discharge was visible in the GR-874 connector.

Although the power measurements described here are admittedly lacking in accuracy, the conclusion that the power dissipated in a multipactor discharge is relatively small seems inescapable. Attempts to measure the

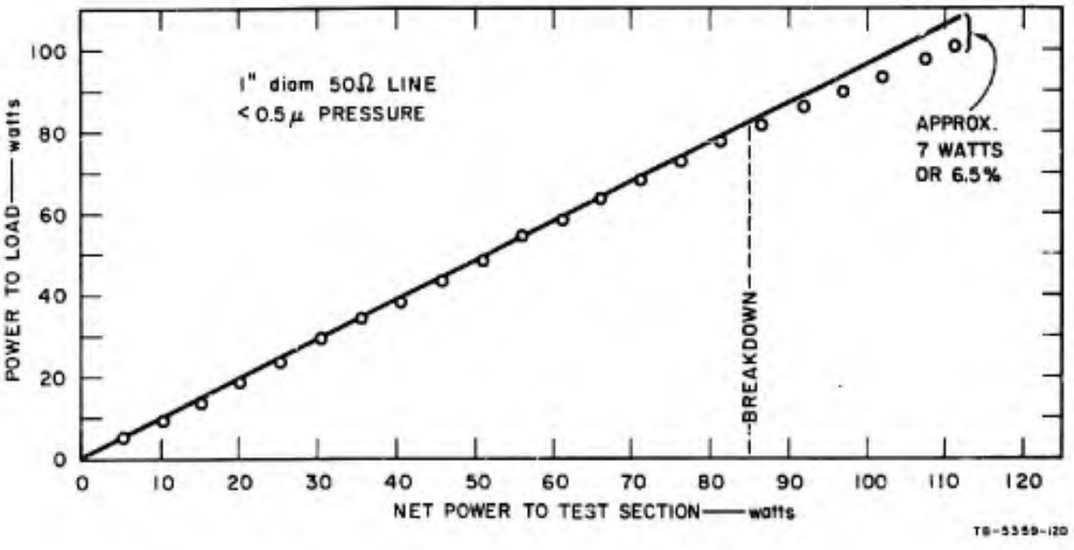

FIG. 15 TRANSMITTED POWER AS A FUNCTION OF NET POWER TO MATCHED TEST SECTION

power dissipated in structures other than long coaxial sections or fairly large parallel-plate electrodes have met with failure when conventional RF-power-measuring techniques were employed, because the multipactor discharge losses were too small to be detected. The effect of the discharge is quite noticeable in high-Q circuits, however. Thus, in the

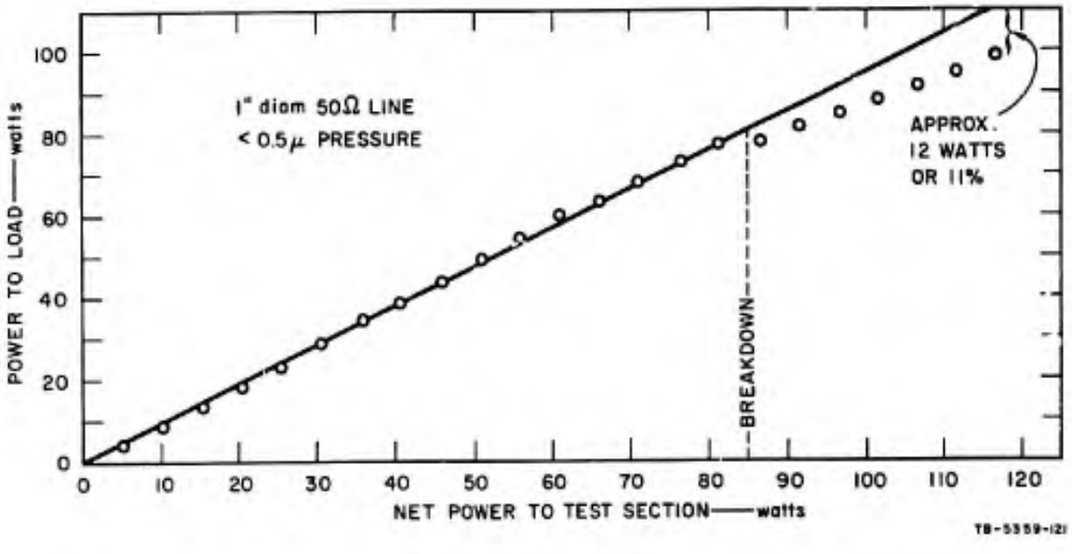

FIG. 16 TRANSMITTED POWER AS A FUNCTION OF NET POWER TO MATCHED TEST SECTION

microwave switch described in Ref. 23, the multipactor discharge is used to detune a cavity; the "arc loss" is only a fraction of a dB. Similarly, in the experiments with parallel-plate geoemtry described in Sec. II, a high-Q tank circuit driven by a low-power signal generator was used to develop the gap-voltage. When the discharge occurs, the tank circuit is detuned and the RF voltage drops noticeably. When such gaps are driven by a low-impedance, high-power source, however, the change in circuit voltage or reflection coefficient is relatively small when the discharge occurs. The only failures on spacecraft that have been definitely attributed to multipactor discharges occurred in high-Q circuits.[27]

C. Other Effects of Multipactor Discharges

Despite the fact that the power loss in a multipactor discharge appears to be relatively trivial unless it occurs in a tuned circuit, the discharge may lead to a more drastic effect through the generation of other failure mechanisms. In the multipactor discharge, for example, all of the power is dissipated in the electrodes, so that these electrodes may become hot enough to melt soft solder. The failure in this case is a mechanical failure, but it would not have occurred without the heating produced by the multipactor discharge. The electrode heating produced by the discharge may also cause significant outgassing (particularly if one of the electrodes is an organic dielectric) so that gas discharges are induced.

Experience with multipacting in two-sided modes suggests that even electrodes that appear to be clean and outgassed may actually have a thin film of oxide on the surface. Experiments with the biased multipactor discharge have illustrated the effects of these films in an interesting manner. Since the oxides are often insulating or only partially conducting, charge can accumulate on the oxide surface and develop very high dc field strengths in the film. When the dielectric strength of the film is exceeded, the film breaks down and a visible flash or scintillation is observed. These scintillations, which are believed to be the same as those described by others in connection with the Malter effect,[28-31] have been observed on the negative electrode when brass or

aluminum electrodes were used. With copper electrodes, however, the scintillations are observed on the positive electrode. It is postulated that the peculiar behavior of copper in this respect results from the fact that the copper cuprous-oxide junction offers little resistance to the flow of electrons from the copper to the oxide, but it impedes the flow of electrons from the oxide to the copper. Electrons or negative ions can thus accumulate on the oxide film and distort the field at the electrode surface of copper electrodes in much the same manner as positive ions are purported to accumulate on the oxides of aluminum and other materials displaying the Malter effect.

Each scintillation is thus a sudden arc discharge of the capacitance of a small region of oxide film or junction. The scintillation discharge is at least a source of noise because of the narrow pulse of high current produced by the discharge. The scintillation discharge may induce more detrimental failure mechanisms, however, such as dc or RF arcs. Furthermore, although the scintillations occur more frequently when dc bias is applied, they also occur without bias.

The association of the scintillation with high-current, low-voltage arc discharges has also been made by Haworth,[32] who experimented with clean electrodes coated with thin insulating films and bombarded with a positive ion beam. Haworth noted that gaps that would not break down under as much as 6000 volts when the voltage was applied while there were no positive ions present, would develop arcs at voltages as low as 34 volts when the ions were present. Westberg[33] also noted cathode scintillations coincident with the transition from glow-to-arc discharge; however, he dismissed them as an effect of the arc rather than the triggering mechanism.

Because the action of the scintillations had been observed in the course of many RF and dc discharge experiments, it was postulated that scintillation-induced arc discharges might be responsible for some of the anomalous electrical activity observed on certain rockets and spacecraft. On rocket vehicles, conditions are particularly favorable for the scintillation-induced arc, since low-impedance, 28-volt dc power

systems are used extensively on these vehicles and low-pressure ionized gases are available from a number of sources, such as rocket motor exhaust, ion engine beam, hot gases from the pyrotechnic systems, bow shock, and even the ionosphere.

In an experiment to demonstrate the feasibility of producing arc discharges with a 28-volt system in a plasma environment, a UG-30C/U RF pressure connector was installed in the base plate of a bell-jar vacuum chamber, and a short aluminum wire was inserted in the center-conductor receptacle of the connector on the vacuum side. On the high-pressure side, the center conductor was connected to the negative terminal of a 28-volt dc source composed of 14 cells of automobile batteries connected in series. The positive terminal of the dc source was connected to the shell of the RF connector. The bell jar was pumped down to about 10 microns Hg, and ionization was produced by an RF discharge at 260 MHz. (The RF power was supplied through a separate connector, so that the only direct connection between the RF and dc systems was a common ground.) When the ionization was produced, an arc formed between the aluminum wire and the connector shell, and very quickly melted and spewed out the center conductor. The center conductor was melted out and removed down to the pressure seal; the seal was destroyed. In one case, a 50-ampere fuse in the dc line was blown by the arc current. Figure 17 shows a connector that was destroyed in the laboratory by a scintillation-induced arc. Adjacent to the damaged connector is a similar connector that was not energized during the experiment.

Similar results were obtained when the experiment was performed using a tinned copper wire or a silver-plated connector pin in place of the aluminum wire. In addition, the experiment was conducted using a 5-ampere regulated dc supply instead of the 28-volt battery. Although the dc supply would not sustain the arc currents, many incipient arcs were observed, and the connector, while not destroyed, was pitted. It appears that the scintillations are a source of electromagnetic interference even when produced by a high-impedance source that precludes the development of an arc. Although good measurements of the energies or spectral content of the scintillations have not been made, it has

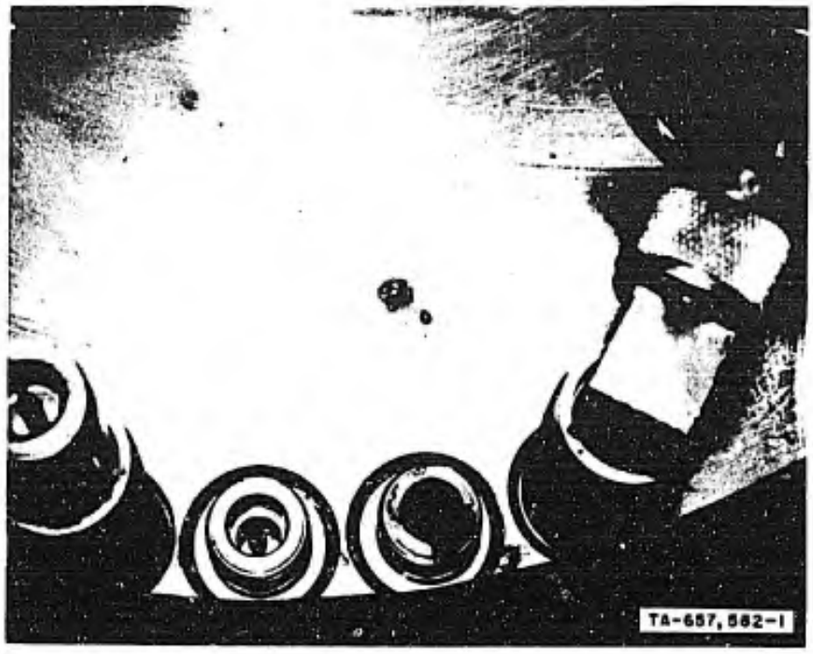

FIG. 17 CONNECTOR DAMAGE CAUSED BY SCINTILLATION-INDUCED ARC DISCHARGE

been found in the course of RF breakdown experiments that the scintillations produce violent swings of a D'Arsonval microammeter used to measure the dc current flow through the discharge region. In one case the reation was sufficient to bend the pointer of the instrument. In a very crude attempt to look at the pulse form, a short electric dipole receiving probe was placed in the vicinity of the scintillation, and the received signal was observed on an oscilloscope. The rise time of the trace appeared to be limited by the bandwidth of the oscilloscope (14 MHz). Other observers have reported rise times of a few nanoseconds for the arcs triggered by the scintillations.[32,33] The scintillation or incipient arc produced under these circumstances may, therefore, have appreciable energy well into the VHF spectrum.

In these experiments, the scintillations were produced by a plasma generated by an RF gaseous discharge rather than by a multipactor discharge. In some recent experiments with high-power RF systems at ionospheric pressures (0.1 to 1.0 μHf) other effects of the scintillation discharge have been observed.[34] In these experiments, scintillation

discharges were produced in an auxiliary electrode system while RF power at 800 MHz was applied to various structures such as baluns, antennas, and transmission lines. In many cases it was observed that the RF components were unaffected by high power at 800 MHz as long as the auxiliary electrodes did not scintillate. However, when a scintillation discharge occurred some 50 cm away, several failure mechanisms, such as multipactor discharges and RF arcs, were induced in the RF structures. Thus, the scintillation discharge, though not destructive of the high-impedance system on which it occurs, may induce catastrophic failure in an adjacent, unrelated system. When scintillation discharges momentarily increase the ionization level at pressures in the 10^{-5} torr range, the multipactor discharge in the high-power structure changed and appeared as an arc causing erosion of the metal surface where it was sustained. It was also found that the outgassing and subsequent increase in pressure, which is caused by the heating of materials following multipactor or arc discharges as well as by high RF currents, can effect a transition of the multipactor discharge to a gas discharge. When the gas discharge occurs, the electrical characteristics are significantly altered.

Thus, as implied earlier, although the multipactor discharge itself seems to be relatively harmless in high-power, low-Q systems, some of the side effects induced by the discharge may have more serious consequences.

IV MULTIPACTOR BREAKDOWN ON DISCONE ANTENNAS

The effect of multipactor discharges on discone antennas was investigated on electrically small discones at 34 MHz using the apparatus illustrated in Fig. 18. Electrically small discones were used because

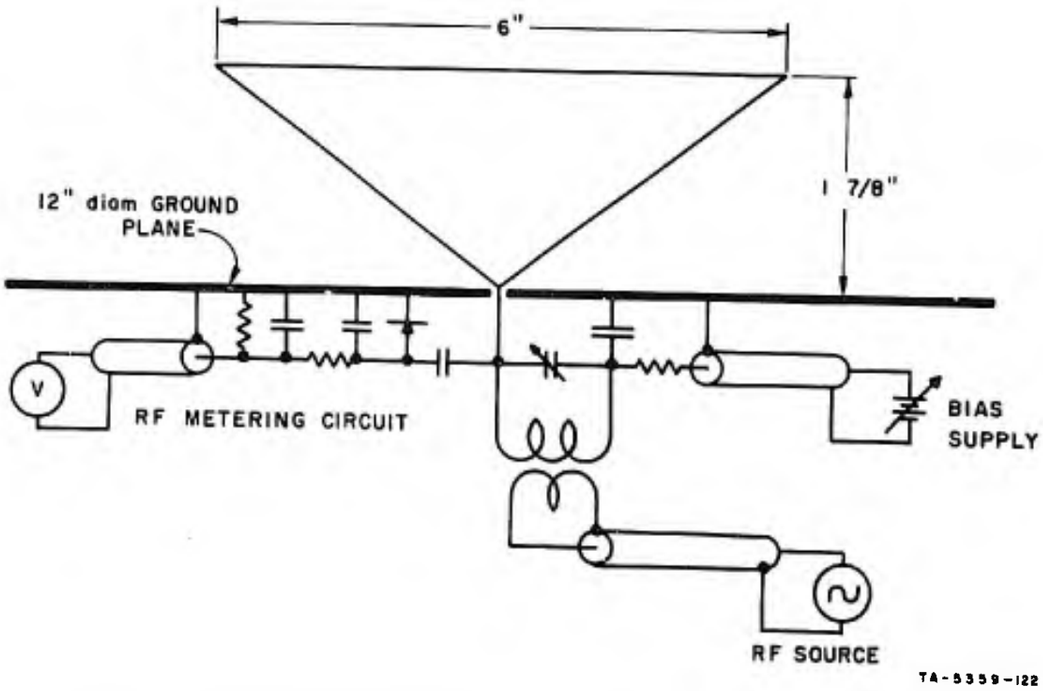

FIG. 18 APPARATUS FOR TESTING DISCONE ANTENNA BREAKDOWN

the multipactor discharge is confined to a region about the feed point where the gap length is proper for the frequency of the RF source. Hence, although the discone antenna is usually electrically large, multipacor discharges would occur only in an electrically small region near the point of the cone.

The measurement technique and metering, bias, and RF coupling circuits were very similar to those used in the coaxial experiments. The cones used in these experiments were formed from copper sheet, and the

12-inch-diameter ground plane was covered with copper sheet. The cones were 6 inches in diameter at the top, as illustrated in Fig. 18. The data shown in Fig. 19 were taken with the top of the cone maintained 1-7/8 inches above the ground plane. Thus, as the cone angle was increased, the height of the apex above the ground plane increased, and for the 180-degree cone angle, the antenna structure was a top-loaded monopole 1-7/8 inches high. Cones narrower than 120 degrees were made with the same slant height as the 120-degree cone and mounted with the apex approximately in the plane of the ground plane.

Contours of RF threshold voltage (rms volts) as a function of dc bias voltage and cone angle are shown in Fig. 19 for these discones. For cone half-angle less than 60-degrees, the discharge voltages were so erratic that smooth contours could not be obtained; even at 60 degrees, the contour is irregular. For cone half-angles less than 30 degrees, even erratic breakdown could not be obtained.

Breakdown could be obtained at cone half-angles as small as 15 degrees when ionization was produced in the bell jar by operating a small auxiliary multipactor discharge at 240 MHz. A discharge initiated on the discone would continue after the auxiliary discharge was stopped, since the discone discharge provided its own ionization once it was initiated. Since the discharge, once initiated, would continue until the RF voltage dropped below the extinguish level, the extinguish voltage was also measured for the narrow cones. These data are shown in Fig. 20. Because the extinguish voltage is the voltage at which the discharge is sustained in its self-generated ionization, it is indicative of the voltage at which a discharge can occur in an environment containing ambient ionization.

In addition to the tests at 34 MHz, brief exploratory tests with discone antennas were also conducted at 57 MHz and at 1200 MHz. At 34 MHz, the multipactor discharge occurred near the edge of the 6-inch-diameter cones when the cone angle was greater than 210 degrees. As the frequency is increased the region of discharge shrinks toward the apex of the cone since the frequency-path-length product must remain approxi-

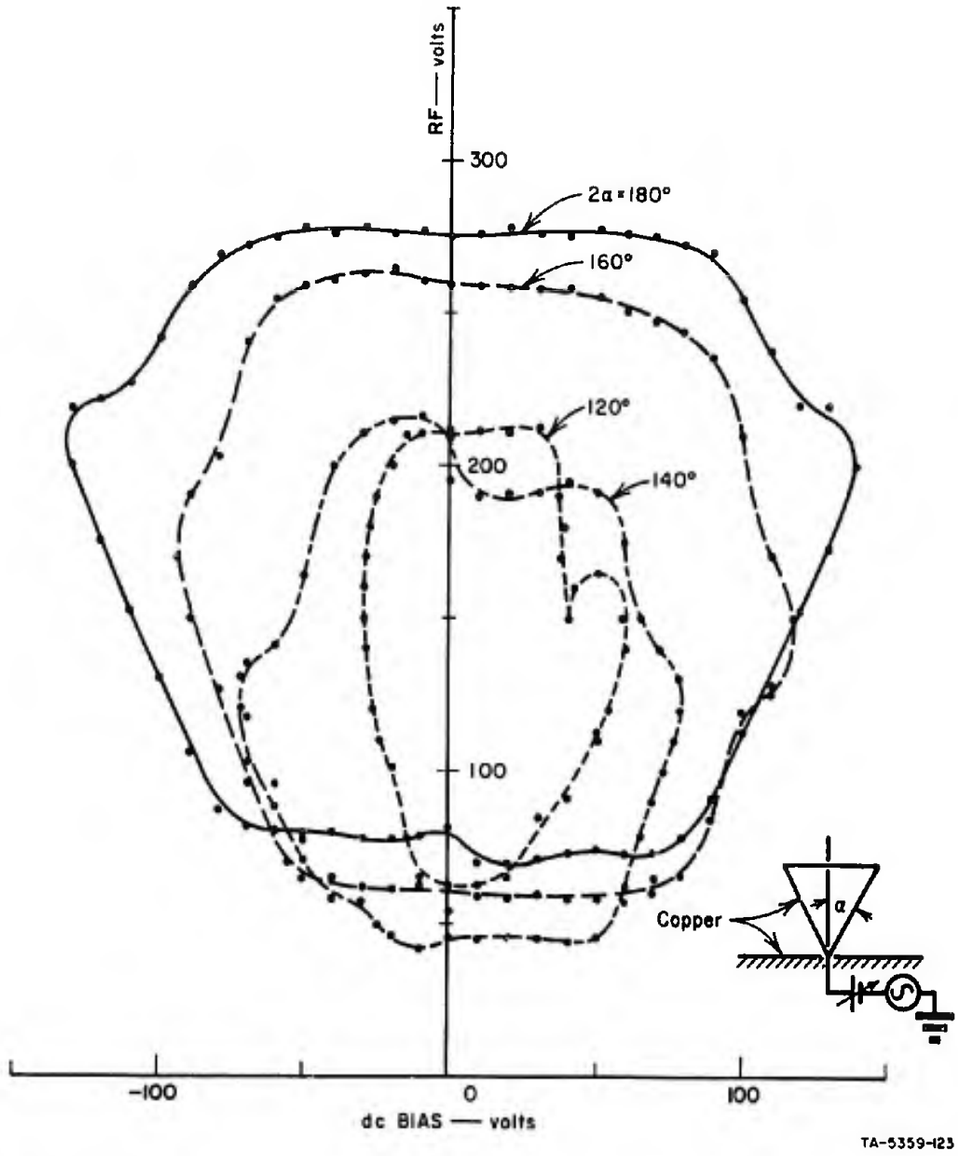

FIG. 19 REGIONS OF MULTIPACTOR DISCHARGE FOR SMALL DISCONE ANTENNAS

mately constant. At 1200 MHz the discharge was confined to a region of about 1-cm radius about the apex of a 120-degree cone. In spite of the fact that the 1200-MHz antenna was well matched to the transmitter, power loss to the multipactor discharge could not be detected on incident and reflected power meter readings; hence the power absorbed by the discharge was apparently of the order of 10 percent, or less, of the radiated

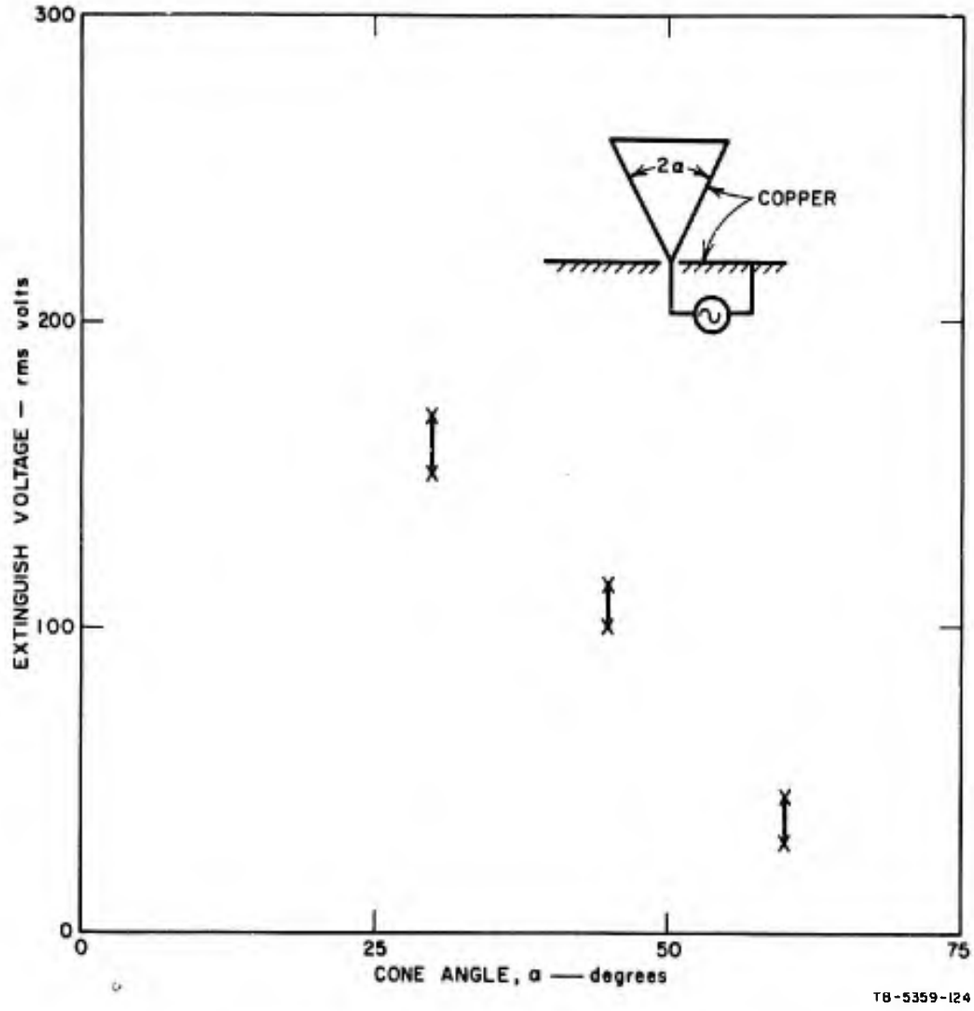

FIG. 20 DISCHARGE EXTINGUISH VOLTAGE FOR SMALL DISCONE ANTENNAS

power. It was also observed that the RF voltage required to initiate the discharge on the discone antenna was relatively independent of frequency.

Another incident that may be of interest occurred during the discone antenna tests. It will be noted in Fig. 18 that the cone was excited by a tuned tank circuit below the ground plane. Initially this circuit was operated in the ambient vacuum of the bell jar, but at the high RF voltages required to explore the upper breakdown threshold, the coil was prone to breakdown. Since the coil is part of the high-Q tank

circuit, this breakdown drastically reduced the voltage applied to the antenna. Since the glow of the discharge was brightest inside the turns, it was first attempted to fill the core of the coil with plastic foam. When this was done, however, the glow appeared on the outside of the turns. The problem was finally solved by imbedding the entire coil in foam. This experience with the tank coil illustrates a case where multipactor discharges in a high-Q circuit can cause system failure. It also illustrates that the multipactor discharge can occur in some non-uniform field geometries that would not at first glance appear to be capable of supporting the discharge. Finally, the cure in the case illustrates one method that may be used to prevent the multipactor discharge--that is, to break up the electron path so that the frequency/path-length product is too small to support the discharge.

BLANK PAGE

V CONCLUSION AND RECOMMENDATIONS

When the work described here was undertaken, it was known that the multipactor discharge occurred in parallel-plane geometries, but it was not known whether it would occur in other geometries, or if so, at what voltages it would occur. It was also known that the discharge could occur in a biased gap, but there were no experimental data available to indicate the effect of bias on the RF threshold or on discharges involving insulated electrodes. The results of the work described in the preceding sections help to supply answers to some of these questions that were previously unanswerable.

It has been demonstrated, for example, that multipactor discharges will occur in a coaxial electrode geometry even if the diameter ratio is very large. The coaxial electrode geometry will support multipactor discharges in the presence of a dc bias, and this electrode geometry will support the one-sided mode of discharge over a large range of bias voltages. The RF threshold for multipactor discharge in the coaxial geometry with large-diameter ratios (>20) and positive bias on the inner conductor was surprisingly low. This was attributed to the peculiar properties of the electron trajectory in the nonuniform field between the electrodes.

The multipactor discharge in a parallel-plate geometry with a variety of electrode materials has also been investigated. The conclusion is that most electrode materials, including insulators, will support multipactor discharges. The only metal tested that would not support multipactor discharges was pure titanium; but a titanium alloy has been shown by Russian experimentors to support the discharge. Lamp black has been used in the laboratory to suppress multipactor discharges, but its effectiveness appears to be degraded by continued ion bombardment. The use of lamp black to suppress multipactor discharges is probably impractical outside the laboratory, since an effective coating is quite fragile--the most effective coatings have been soft, fluffy coatings

obtained by smoking the surface with an acetylene flame. The use of insulation over metal electrode surfaces does not prevent the discharge from occurring since the secondary emission from insulating materials is usually better than from metals. The use of insulated electrodes does lead to some interesting electrostatic phenomena if the gap is biased or can become biased due to nonuniform fields.

The attempts to measure the power dissipated in the multipactor discharge have resulted in more of a qualitative conclusion than a quantitative conclusion. The power dissipated in the discharge was too small to measure accurately in the presence of other circuit losses. The power dissipated in the discharge is thus small in terms of the power per unit cross section area of discharge region. Yet this power, which is all dissipated in the electrodes, is sufficient to melt soft solder joints in the vicinity of the discharge. The power loss in the discharge is most noticeable, however, when it occurs in a high-Q circuit. Here the discharge absorbs enough power to detune the circuit and produce a significant voltage drop. Although the power absorbed by the discharge is small and is known to be a problem primarily in high-Q circuits, the electrode heating and surface effects produced by the discharge may also lead to other failure mechanisms even in low-Q, low-impedance circuits. These failures may be associated with accelerated outgassing from the electrodes or scintillation discharges on the electrode surfaces.

The experiments with the discone antennas indicate that multipactor discharges can occur in the wide-angle discone geometry, but that the power loss in the discharge is a small fraction of the radiated power. As indicated above, the primary concern appears to be with secondary failure mechanisms induced by the multipactor discharge rather than with the direct effects of the discharge on antenna performance.

For the designer of RF components for space, an awareness of the effects of multipacor discharges and of the conditions under which they occur will be necessary if his components are to perform reliably in the space environment.

An awareness of the threat of multipactor breakdown will permit anticipation of the features of the component that will most obviously invite multipactor breakdown. Often, relatively minor design changes can be incorporated to minimize the probability of a discharge occurring or of damage being incurred if the discharge does occur. Since the unexpected is prone to occur in any new design or new application of an old design, however, RF components for space should be tested in the space environment to ascertain that multipactor discharges do not affect the performance of the component, or the system of which the component is a part, or other "independent" systems on the spacecraft.

In the space environment for such testing, the ambient ionization of space (e.g., the ionosphere), as well as the pressure, should be simulated. For some space applications it might be necessary to simulate additional environmental factors such as those influencing outgassing and spacecraft contamination, and perhaps solar radiation. There is little information by which to judge the effect these factors might have on multipactor discharges; further investigation in these areas appears to be required.

The theory of the multipactor discharge is reasonably well developed only for the uniform field gap in the absence of bias and before the electron density has built up to the point where space charge affects the electron trajectory. Further effort could profitably be devoted to extending these bounds by more careful measurements of the power dissipated, and a correlation of this power with the number and energy of electrons participating in the discharge. These measurements should be supplemented with a more comprehansive analysis of the discharge after build-up to obtain a better understanding of the power dissipated in the discharge and the implications of this power on the system response.

Also of interest in determining the physics of the discharge is a better understanding of the distribution of the electrons in the gap. That is, are the electrons in a sheet, as often assumed, or are they distributed throughout the permissible emission phase angles, as the stability criteria suggest? A more refined pill-box measurement would be helpful in assessing the electron distribution during build-up and after it is established, and in determining the effect of bias on the distribution.

REFERENCES

1. J. D. Cobine, Gaseous Conductors (Dover Publications, Inc., New York, N.Y., 1958).

2. F. Kossel and K. Krebs, "Die Pendelvervielfachung von Sekundarelektronon (Multipactoreffeckt) als Zundbedingung von Hochfrequenzentladungen," Z. Physik 175, pp. 382-390 (1963).

3. A. J. Hatch and H. B. Williams, "The Secondary Electron Resonance Mechanism of Low-Pressure High-Frequency Gas Breakdown," J. Appl. Phys., 25, pp. 417-423 (April 1954).

4. A. J. Hatch and H. B. Williams, "Multipacting Modes of High-Frequency Gaseous Breakdown" Phys. Rev. 112, pp. 681-685 (November 1958).

5. H. Alfven and H. J. Cohn-Peters, "Eine neue Art von Hochfrequenz-Entladung im Vakuum und deren Verwendung als Ionenquelle," Arkiv for Matematik, Astronomi och Fysik, 31A, pp. 1-17 (1944).

6. E. W. B. Gill and A. von Engel, "Starting Potentials of High-Frequency Gas Discharge at Low Pressure," Proc. Roy. Soc. (London) A192, pp. 446-463 (February 1948).

7. G. Francis and A. von Engel, "The Growth of High-Frequency Electrodeless Discharge," Trans. Roy. Soc. (London) 246A, pp. 143-180 (July 1953).

8. A. J. Hatch, "Electron Bunching in the Multipacting Mechanism of High-Frequency Discharge," J. Appl. Phys. 32, pp. 1086-1092 (June 1961).

9. A. Miller, H. B. Williams, and O. Theimer, "Secondary-Electron-Emission Phase-Angle Distributions in High Frequency Multipacting Discharges," J. Appl. Phys. 34, pp. 1673-1679 (June 1963).

10. K. Krebs, "Uber die Pendelvervielfachung von Sekundarelektronen in Hochfrequentzfeldern," Z. Angew Phys. 2, pp. 400-411 (October 1950).

11. K. Krebs and H. Meerbach, "Die Pendelvervielfachung von Sekundarelektronen," Ann. Physik 15, No. 3-4, pp. 189-206 (1955).

12. K. Krebs and H. Meerbach, "Die Elektronendichte und Geschwindigkeitsverteilung bei der Pendelvervielfachung von Sekundarelektronen," Ann. Physik, 18, pp. 146-162(August 1956).

13. K. Krebs, "Frequenzvervielfachung im Zentimeterwellengebiet durch Sekundarelektronen," Z. Physik, 154, pp. 19-26 (January 1959).

14. K. Krebs and H. V. Villiez, "Die Anregung von Hohlraumresonatoren durch Pendelvervielfachung von Sekundarelektronen," Z. Physik, 154, pp. 27-33 (January 1959).

15. F. Kossell and K. Krebs, "Die Pendelvervielfachung von Sekundarelektronen im Dezimeterwellengebiet," Z. Physik, 170, pp. 165-175 (1962).

16. E. F. Vance, "One-Sided Multipactor Discharge Modes," J. Appl. Phys. 34, pp. 3237-3242 (November 1963).

17. E. F. Vance and J. E. Nanevicz, "One-Sided Multipactor Discharge Modes," Tech. Report 75, Contract AF 19(628)-325, SRI Project 3977, Stanford Research Institute, Menlo Park, California (April 1963).

18. C. Milazzo, "Study of Multipactor Discharge in the Presence of a D-C Bias," Tech. Memo. TM-61-15, General Electric Company, Palo Alto, California (March 13, 1961).

19. B. A. Zager and V. G. Tishin, "Multipactor Discharge and Ways of Suppressing It," Soviet Phys. Tech. Phys., 9, pp. 234-241 (1964).

20. W. G. Abraham, "Interactions of Electrons and Fields in Cavity Resonators," Ph.D. dissertation, Stanford University, Stanford, California (1950).

21. D. H. Preist, "Multipactor Effects and Their Prevention in High-Power Microwave Tubes," Microwave J., 6, pp. 55-60 (October 1960).

22. D. H. Preist and R. C. Talcott, "On the Heating of Output Windows of Microwave Tubes by Electron Bombardment," Trans. IRE ED 8, pp. 243-251 (July 1961).

23. M. P. Forrer and C. Milazzo, "Duplexing and Siwtching with Multipactor Discharges," Proc. IRE 50, pp. 442-450 (April 1962).

24. H. Bruining, Physics and Applications of Secondary Electron Emission (Pergamon Press Ltd., London, 1954).

25. Kees Bol, "The Multipactor Effect in Klystrons," 1954 IRE National Convention Record 2, pp. 151-155.

26. R. Woo, "Experimental Study of Multipacting Between Coaxial Electrodes," Space Programs Summary, Vol. IV, pp. 37-41, Jet Propulsion Laboratory, California Institute of Technology, Pasadena, California (October 1966).

27. H. W. Street, "High Voltage Breakdown Problems in Goddard Scientific Satellites," JPL Tech. Memo. 33-280, Jet Propulsion Laboratory, California Institute of Technology, Pasadena, California (December 1966).

28. L. Malter, "Anomalous Secondary Electron Emission, a New Phenomenon," Phys. Rev. 49, p. 478 (1936).

29. L. Malter, "Thin Film Field Emission," Phys. Rev. 50, p. 48, (1936).

30. L. R. Koller and R. P. Johnson, "Visual Observations of the Malter Effect," Phys. Rev. 52, p. 519 (1937).

31. L. B. Griffiths, "The Arcing Behavior of Metals in Contact with a Low-Energy Hydrogen Plasma," J. Nuclear Matls. 4, pp. 30-36 (1961).

32. F. E. Haworth, "Experiments on the Initiation of Electric Arcs," Phys. Rev. 80, pp. 223-226 (1950).

33. R. G. Westberg, "Nature and Role of Ionizing Potential Space Waves in Glow-to-Arc Transitions," Phys. Rev. 114, pp. 1-17 (1959).

34. J. B. Chown and G. August, "Power-Handling Capability of Radiating Systems in the Exoatmosphere," Tech. Reports 1 and 2, Contract AF 19(628)-5167, Subcontract 324, SRI Project 5609, Stanford Research Institute, Menlo Park, California (October 1966, September 1967).